

HYDROCARBON GENERATION AND MIGRATION FROM SUB-THRUST SOURCE ROCKS TO FORELAND RESERVOIRS: THE AUSTRIAN MOLASSE BASIN

Jürgen GUSTERHUBER¹⁾²⁾, Ralph HINSCH³⁾⁴⁾, Hans-Gert LINZER³⁾ & Reinhard F. SACHSENHOFER¹⁾

¹⁾ Montanuniversität Leoben, Department Applied Geosciences and Geophysics, Chair of Petroleum Geology,

Peter-Tunner-Straße 5, A-8700 Leoben, Austria;

²⁾ Present address: SANTOS Ltd., 60 Flinders Street, Adelaide SA 5000, Australia;

³⁾ RAG Rohöl-Aufsuchungs Aktiengesellschaft, Schwarzenbergplatz 16, A-1015 Vienna, Austria;

⁴⁾ Present address: OMV Exploration & Production GmbH, Trabrennstraße 6-8, 1020 Vienna;

¹⁾ Corresponding author, juergen.gusterhuber@santos.com

KEYWORDS

hydrocarbon migration
petroleum system
Molasse Basin
modelling

ABSTRACT

The present study shows structural and petroleum systems models investigating the hydrocarbon potential of the central part of the Austrian Molasse Basin.

The structural model is based on kinematic modeling with pseudo-geodynamic background. It reflects the structural evolution of the frontal and adjacent orogenic wedge and serves as input for the basin and petroleum systems models. Total tectonic shortening in the forward modeled section is 48.5 km, corresponding to 69% of shortening.

The reconstructed paleo heat flow based on maturity data is low (32 - 26 mW/m²) and decreases southwards towards the orogen. Formation temperatures suggest that present-day heat flows decrease in the same direction from 52 to 37 mW/m². Most probably heat flow is increased during Pliocene and Pleistocene times.

A combination of 'paleo' and 'present day' heat flow scenarios was used for the calculation of hydrocarbon generation along a N-S trending section crossing the Sierning imbricates. According to these models, hydrocarbon generation commenced during the Early Miocene at about 18 Ma due to deep burial beneath Alpine nappes and was terminated during the Late Miocene (~ 8 Ma) due to cooling caused by uplift and erosion. About 40 % of the total source potential was realized beneath the Northern Calcareous Alps in the Molln 1 Well area.

Hydrocarbon migration commenced contemporaneously with hydrocarbon generation, but continues until present day. Despite of model simplifications, the 2D migration model reflects important processes confirming previous interpretations. Amongst these are: (1) oil migration across faults from the Oligocene source rocks into stratigraphically deeper carrier/reservoir beds; (2) long-distance (>50 km) lateral migration of oil (and gas); (3) migration of gas along fault zones into the Sierning imbricates; (4) vertical migration of gas into the Puchkirchen and Hall formations, probably as a result of uplift and pressure reduction.

Results of a 'pseudo 3D' flow path model show that absence of commercial accumulation in the western part of the study area is not a result of missing structures, but of the absence of hydrocarbon charge. The mismatch between observations and model results also highlights the important role of fault zones as migration pathways.

'Palaeopasteurization' of shallow reservoirs may explain that biodegradation in the Austrian part of the Alpine Foreland Basin is limited to the depth interval down to 800-1000 m sub-sea.

Die vorliegende Arbeit zeigt Struktur- und Kohlenwasserstoffsystem-Modelle, welche das Potential des zentralen Teils des österreichischen Molassebeckens erforschen.

Das strukturgeologische Modell schließt die Entwicklung des erweiterten nördlichen Randes des alpinen Orogens mit ein und dient gleichzeitig als Grundlage fuer das Beckenmodell. Die tektonische Verkürzung im Modell wurde mit 48.5 km angenommen, was 69 % Gesamtverkürzung entspricht.

Der rekonstruierte Paläowärmeffluss, basierend auf Reifedaten, ist relativ niedrig und nimmt von Norden nach Süden ab (32 – 26 mW/m²). Der errechnete heutige Wärmeffluss welcher auf gemessenen Formationstemperaturen basiert, nimmt ebenfalls von Norden nach Süden ab, wenn auch auf höherem Niveau (52 – 37 mW/m²). Wahrscheinlich nahm der Wärmeffluss während des Pliozäns oder Pleistozäns zu.

Eine Kombination aus diesen beiden Wärmefflusszenarien diene als Grundlage für die Modellierung der Kohlenwasserstoffgeneration entlang eines 2D Profiles in der Sierninger Schuppenzone. Die Modelle zeigen, daß die ersten Kohlenwasserstoffe vor rund 18 Millionen Jahren gebildet wurden und dieser Prozeß vor rund 8 Millionen Jahren zu Ende war. Diese Zeitabfolge kann direkt mit der tiefen Versenkung des Deckenstapels unter die Alpen, gefolgt von nachfolgender Hebung und Erosion vor rund 8 Millionen Jahren, in Verbindung gebracht werden. Ungefähr 40 % des gesamten Muttergesteinspotentials wurden im südlichen Bereich des Profiles unterhalb der Nördlichen Kalkalpen im Bereich der Bohrung Molln1 realisiert.

Die Migration der Kohlenwasserstoffe setzt gleichzeitig mit der Bildung derselben ein und bleibt bis heute aktiv. Trotz notwendiger Vereinfachungen im Modell können mit dem 2D Migratinonsmodell viele Prozesse, welche in früheren Studien bereits als möglich erachtet wurden, visualisiert werden. Diese sind unter anderem: (1) Ölmigration entlang von Störungen von oligozänen Mutterge-

steinen in stratigraphisch tiefere Träger- und Reservoirhorizonte; (2) ausgedehnte (>50 km) laterale Migration von Öl und Gas; (3) Gasmigration entlang von Störungszonen in den Bereich der Sierninger Schuppenzone; (4) vertikale Migration von Gas in die Puchkirchen und Hall Formation, welche möglicherweise ein Ergebnis von Hebung und Druckreduktion ist.

Ein auf Strukturkarten basierendes „Pseudo 3D“ Fließmodell zeigt, daß das tatsächliche Nichtvorhandensein von kommerziell nutzbaren Petroleumakkumulationen im westlichen Teil des Untersuchungsgebietes auf fehlende Muttergesteine, und nicht auf fehlende Störungsstrukturen zurückzuführen ist.

Die Diskrepanz zwischen Beobachtungen und Modelliererergebnissen zeigt zugleich den großen Einfluss von Störungszonen, welche als Migrationspfade dienen.

„Paläopasteurisierung“ von seichten Gaslagerstätten ist eine mögliche Erklärung dafür, daß Biodegradation im österreichischen Teil des alpinen Vorlandbeckens auf eine Tiefe von ungefähr 800 – 1000 m (unter Meereshöhe) begrenzt ist.

1. INTRODUCTION

The Molasse Basin represents the foreland basin at the northern edge of the Alps (Fig. 1). The basin fill consists of Mesozoic and Cenozoic rocks overlying the crystalline basement of the Bohemian Massif (Malzer et al., 1993). Petroleum exploration has been successful for decades. Hence the basin is considered to be mature in terms of petroleum exploration (Veron, 2005). Two reasonably well understood petroleum systems can be distinguished in the investigated area of the basin (Wagner, 1996, 1998): (1) a thermogenic oil system related to Lower Oligocene source rocks (Schmidt and Erdogan, 1993; Schulz et al., 2002; Sachsenhofer and Schulz, 2006; Gratzer et al., 2011), and (2) a biogenic dry gas system located in Oligo-/Miocene sediments (Schulz and van Berk, 2009; Schulz et al., 2009; Reischenbacher and Sachsenhofer, 2011). Previous basin modeling approaches (Schmidt and Erdogan, 1993, 1996) showed that oil and thermogenic gas was formed underneath the Alpine nappes and migrated laterally to the north.

The distribution of gas deposits in the Molasse Basin is an outcome of several complex processes. Hence, there are still a lot of pending issues concerning generation, migration and alteration of hydrocarbon gases. For instance gas from Oligo/Miocene reservoirs, interpreted as biogenic in origin, may show geochemical signatures of thermal gas and locally even contains liquid hydrocarbons. This indicates migration of thermogenic hydrocarbons from deeper to shallower horizons and mixing of both petroleum systems (Reischenbacher and Sachsenhofer, 2011).

The stratigraphic evolution of the tectonically mainly undeformed foreland is relatively well constrained by hundreds of wells drilled and 3D seismic data (e.g. Linzer, 2001; De Ruig and Hubbard, 2006; Hinsch, 2008; Hubbard et al., 2005, 2009). In contrast, the folded and imbricated southernmost part is still poorly understood and the hydrocarbon potential is not fully explored. First attempts to a better understanding of the folded and imbricated southernmost part of the basin were made by Linzer (2001, 2002, 2009) and Covault et al. (2009). New wells and continued seismic acquisition improved the knowledge in the kinematic evolution and the understanding of the hydrocarbon generation potential of the latter in recent times (Gusterhuber et al., in press; Hinsch, 2013). Within the Austrian part of the basin, different regions of imbricated zones can be distinguished based on different structural architecture and kinematics. The Sierning imbricates represent the eastern-

most piece of these imbricated zones (Fig. 1) (Hinsch and Linzer, 2010). Due to different timing of tectonic processes, the stratigraphic position of the decollement varies between the eastern and the western basin region. While Upper Cretaceous marls act as detachment horizon in the western part of the area (Perwang imbricates), the decollement is located above Lower Oligocene source rocks in the Sierning imbricates and in the Regau overthrust segment. Therefore, occurrence of source rocks within the thrust sheets is restricted to the Perwang imbricates. Gusterhuber et al. (in press) showed (based on modeling results and geochemical data) that source rocks at least in deeper parts of the Perwang imbricates reached the oil window.

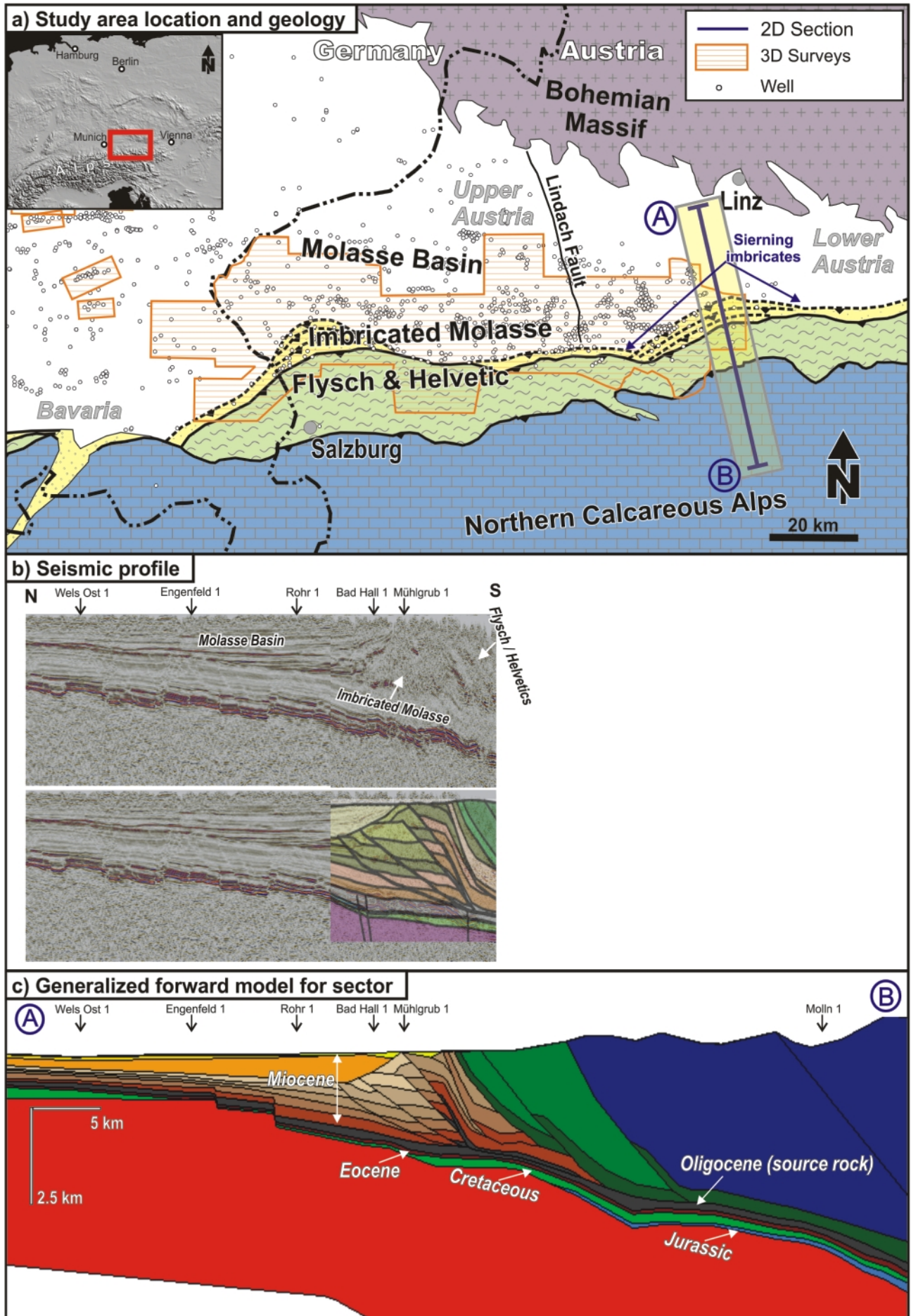
The aims of this study are to investigate hydrocarbon generation in the Alpine sub-thrust and hydrocarbon migration into the undeformed foreland. In addition the study addresses biodegradation and mixing processes of gas. To achieve these goals, a two-dimensional basin and petroleum systems model was established crossing the Sierning imbricates in the eastern part of the study area. Structure maps of the main reservoir horizons have been used to show possible hydrocarbon migration pathways in map view.

The geometry of the thermal basin model is based on a structural forward model. Application of forward modeling was essential to consider the complex evolution of the thrust sheets. Also, the Molasse Basin was subjected to recent erosion and uplift events which represent an additional challenge in terms of basin modeling. This effect was considered in the thermal basin model using data from Gusterhuber et al. (2012).

2. GEOLOGICAL EVOLUTION

The Northern Alpine (Molasse) Foreland Basin of Austria

FIGURE 1: a) Simplified geological map of the study area (outline of the imbricated Molasse from the subsurface); course of the 2D section (A – B) in the Sierning imbricates as well as the area for which the structural model is considered valid and where the thermal model may have significance to have a similar thermal history (yellow shading); wells (approx. status 2010); the inset map (top left) shows the position of the study area on a shaded relief in the frame of Central Europe. b) 2D seismic section; interpretation overlay including calibration wells and main geotectonic units c) generalized structural forward model considered to be valid for the specified corridor and important stratigraphic units (e.g. Eocene reservoir rocks: orange; source rocks: dark grey).



and Bavaria was formed due to collision of the Alps with the southern margin of the European platform during the middle Paleogene (Röder and Bachmann, 1996; Sissingh, 1997) and represents a typical asymmetric foreland basin in terms of an increasing basin depth toward the Alpine thrust front in the south. The basement of the Molasse trough is formed by crystalline rocks of the Bohemian Massif as part of the European continental margin. Mesozoic evolution started with the deposition of Jurassic sandstones and platform carbonates as well as Upper Cretaceous sandstones and marls (Fig. 2). Following on a major uplift and erosion event during the latest Cretaceous and earliest Paleogene, the Paratethys Sea transgressed progressively on a peneplain during the latest Eocene. The onset of Molasse sedimentation is characterized by Upper Eocene fluvial to shallow marine sandstones and limestones. Basically, the Cenozoic basin fill can be subdivided into autochthonous and allochthonous Molasse units (Steininger et al., 1986). Relatively undisturbed autochthonous units overlie either crystalline basement or Mesozoic rocks. Allochthonous units comprise the Molasse imbricates and are composed of rocks which were incorporated in the Alpine thrusts during tectonic movements.

During the earliest Oligocene the area subsided rapidly (Genser et al., 2007) to deep water conditions (approx. 800 m; Dohmann, 1991) with the deposition of often organic rich fine grained sediments. Flexural bending of the European plate due to the collision with the Alpine wedge led to reactivation of pre-Cenozoic NNW-SSE trending faults and to the development of E-W (south and north dipping) normal faults being mainly active in early Oligocene times (Wagner, 1996, 1998; Nachtmann, 1995).

During the Late Oligocene and earliest Miocene the continued northward movement of the Alps caused the formation of the Molasse imbricates and increased sediment discharge from the south (Kuh-lemann and Kempf, 2002). Fully marine conditions prevailed in the basin up to the Early Miocene and deep water channel systems developed from W to E along the basin axis, filling the Puchkirchen trough (Linzer, 2002; De Ruig and Hubbard, 2006). This channel belt represents a mixed depositional system consisting of debris flows and turbidity currents (Bernhardt et al., 2012). Towards the northern border of the basin, deep

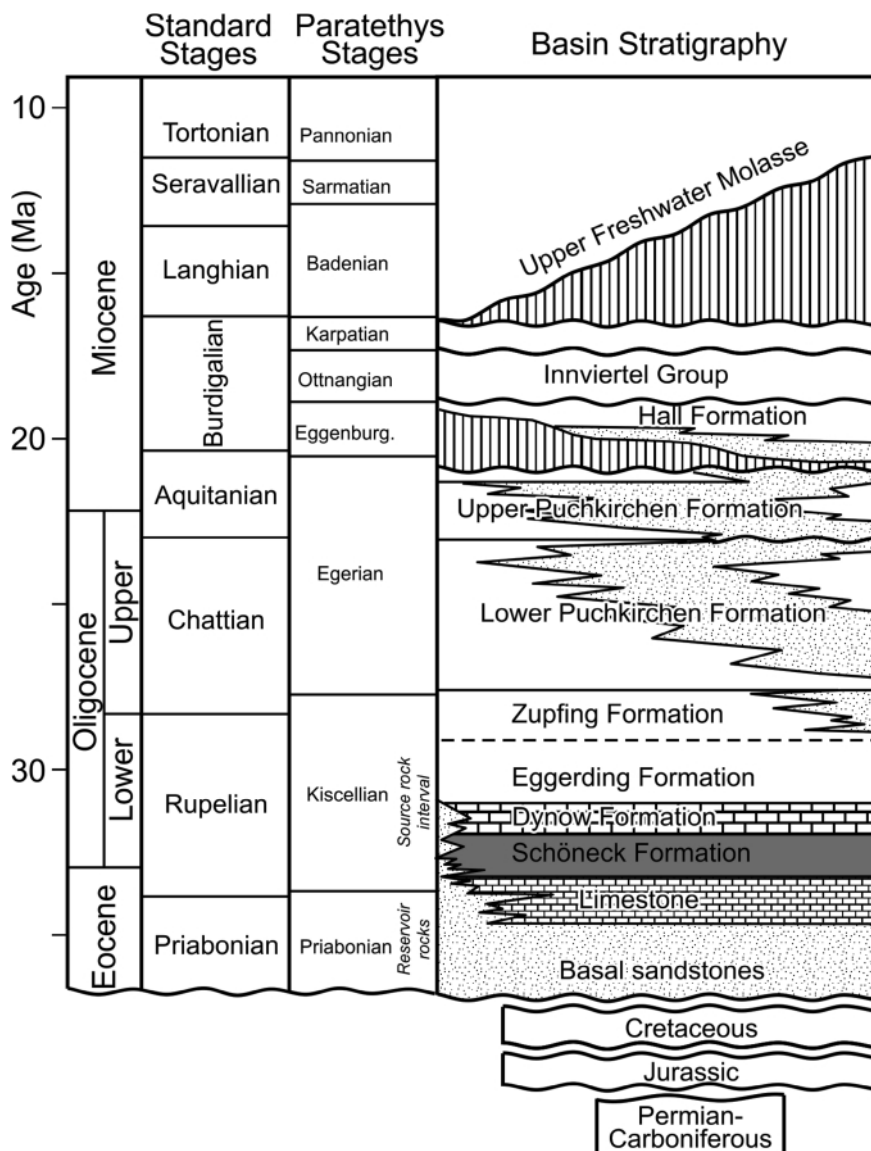


FIGURE 2: Stratigraphy of the Austrian part of the Molasse Basin (modified from Wagner, 1998).

marine sediments graded into brackish sands, clays and minor coal bearing successions (Krenmayr, 1999). At the same time terrestrial coarse grained sediments have been deposited on top of the Alpine wedge, the Augenstein Formation of the Northern Calcareous Alps (NCA) region (Frisch et al., 2001).

The lower part of the Eggenburgian Hall Formation (Fig. 2) is still dominated by deep-water deposits. Later, prograding deltas indicated the transition to shallow marine conditions and filled the accommodation space of the basal Hall trough (Hubbard et al., 2009; Grunert et al., 2013). Upper Burdigalian sediments of the overlying Innviertel Group are represented by tide dominated silts and brackish-fluvial sands (Rögl, 1998; Grunert et al., 2012).

Subsequently, a several hundred meters thick succession composed of coal-bearing clays, sands and fluvial gravels (Upper Freshwater Molasse) was deposited following on a hiatus. Today these Middle/Upper Miocene sediments are largely eroded due to post-depositional uplift over the last 9 m.y. (Genser et al., 2007; Gusterhuber et al., 2012).

3. PETROLEUM SYSTEMS

So far two different petroleum systems have been distinguished in the Austrian part of the Molasse Basin: (1) a Lower Oligocene to Mesozoic thermally generated oil and gas system and (2) an Oligocene-Miocene biogenic gas system (Wagner, 1996, 1998).

(1) The most important reservoir for oil and minor thermal gas are Upper Eocene basal sandstones (Fig. 2). Additional hydrocarbons are trapped in Upper Eocene limestones as well as in Upper Cretaceous glauconite sandstones and Lower Oligocene horizons (Malzer et al., 1993). Most thermal oil and gas prospects in the Molasse Basin are bound to fault systems featuring several hundred meters of vertical throw (Nachtmann, 1995). Some shallow Molasse oils from northern reservoirs are classified as heavily biodegraded (Gratzer et al., 2011). Reischenbacher and Sachsenhofer (2011) assume that gas in shallow Eocene reservoirs south of Linz has been formed by anaerobic biodegradation of pre-existing oil accumulations.

Potential source rocks are restricted to the Lower Oligocene succession and comprise (from bottom to top): Schöneck Formation, Dynow Formation and Eggerding Formation (Fig. 2; Tab. 1; Schulz et al., 2002; Sachsenhofer et al., 2010). The deeper-water organic rich shales and marls of the Schöneck Formation have the highest source potential. The overlying Dynow Formation is composed of three sedimentary cycles, each starting with marlstones and grading into organic shales (Schulz et al., 2004). The Eggerding Formation is composed of grey laminated pelites with thin white-colored layers of calcareous nannoplankton (Sachsenhofer et al., 2010). The Eggerding Formation is overlain by the Zupfing Formation consisting of clay marl. Only the lower part of the latter 150 m thick succession is rich in organic matter. Present-day distribution of Lower Oligocene rocks is controlled by submarine erosion which affected the northern passive slope of the foreland basin west of the Lindach Fault (Fig. 1) where sediments were removed gravitationally after their deposition from the northern slope and re-deposited in deeper basin areas. Later, these re-deposited organic rich rocks (termed Oberhofen facies) were overridden by the Alpine nappes (Sachsenhofer et

al., 2010). In contrast, lower Oligocene units with a normal source rock facies in autochthonous successions have been encountered in wells east of the Lindach Fault (Sachsenhofer and Schulz, 2006; Sachsenhofer et al., 2011).

(2) Isotopically light gas was probably generated by bacterial activity in Oligocene and Miocene shales (Malzer et al., 1993; Schulz and van Berk, 2009). Based on gas wetness and isotope data, Reischenbacher and Sachsenhofer (2011) described mixing of biogenic and thermogenic hydrocarbons including condensate.

The bacterial gas is associated with thermally immature potential source rocks which contain more than 0.5 % TOC. The reservoirs and source rocks are intimately connected (Schulz et al., 2009). Productive reservoirs are found in different subsurfaces of the Puchkirchen and Hall channel systems (De Ruig and Hubbard, 2006; Hubbard et al., 2009).

4 METHODOLOGY

4.1 CROSS SECTION FORWARD MODELING

Hinsch (2013) analyzed the kinematic evolution of the imbricated Molasse based on 3-D seismic and well data interpretation as well as section balancing. For the Sierning imbricates, a retro-deformed section was presented. For the present study a forward model of Alpine wedge advance and Molasse imbrication is established of which 10 time steps are used. The forward modeling approach allows to include eroded sediments and early evolutionary stages that otherwise would not be represented by an individually balanced and restored section. The same methodology was already successfully used for a section through the Perwang imbricates approx. 80 km further to the west of the Sierning section (Gusterhuber et al., in press).

The software package LithoTect (Landmark-Halliburton) is used for forward modeling, utilizing standard integrated fault-slip algorithms. The time span considered in the forward model is early Oligocene to present. Individual model steps are generated after each deformation increment and manual editing to include subsidence, erosion and syntectonic sedimen-

Formation	Av. Thickness [m]	TOC [%]	HI [mgHC/gTOC]
Eggerding Formation	35 - 50	1.5 - 6.0	250 - 400
Dynow Formation	5 - 15	0.5 - 3.0	500 - 600
Schöneck Formation	10 - 20	2.0 - 12.0	400 - 600
Merged source rock interval		2	450
,Oberhofen facies'	~50	~1.3	400

TABLE 1: Characteristics of Lower Oligocene source rocks (Schulz et al., 2002; Sachsenhofer and Schulz, 2006; Sachsenhofer et al., 2010). TOC: total organic carbon; HI: hydrogen index.

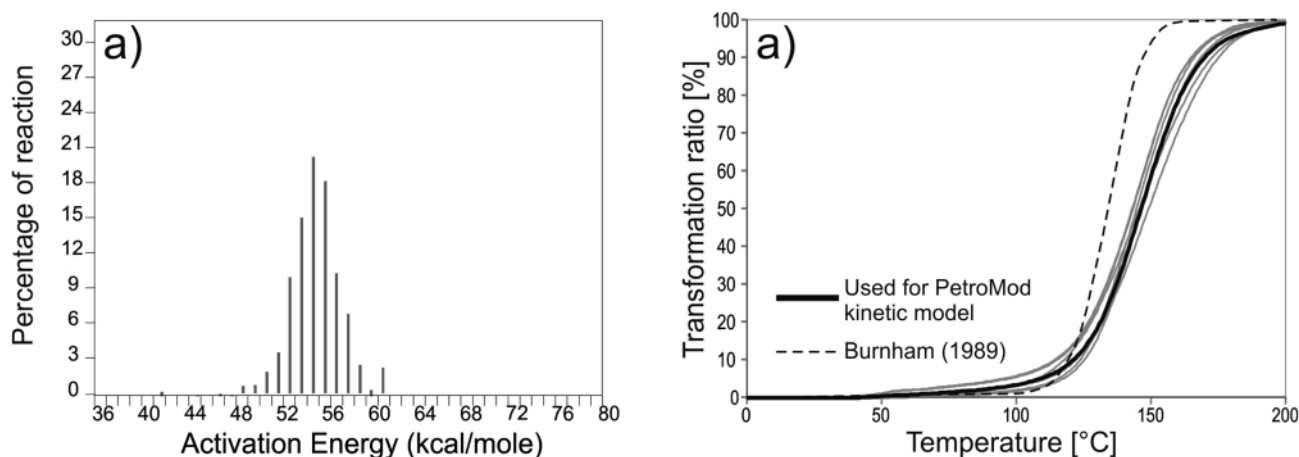


FIGURE 3: a) Kinetic parameters which were used to model petroleum generation; b) Predictions of transformation ratio for five different Lower Oligocene source rock samples based on kinetic parameters and a heating rate of 3.3 °C/million years. The prediction for the sample selected for modeling is shown by a thick black line. The dashed line represents predictions for a Type II kerogen (Burnham, 1989), which was used for sensitivity analysis.

tation. The resulting time steps are later merged into the TecLink basin model of PetroMod (Schlumberger).

In LithoTect the forward modeling was done only on a kinematical basis. However, in order to reflect a more realistic, pseudo-dynamic evolution, the section was manually modified to comply with geodynamically plausible geometries. Subsidence, erosion and syntectonic deposition are added after each deformation increment in order to match the known or plausible paleo-geographic conditions like facies distribution and water depth.

The presented model thus can be termed kinematic model with geodynamic background and compares to the approach used in Gusterhuber et al. (in press). Fully geodynamic modeling is far beyond the scope of this study. In addition, too many parameters for a full dynamic simulation are unknown or uncertain, and thus, results would not be more accurate.

4.2 THERMAL BASIN MODELING

Basin modeling integrates geological, geophysical and geochemical properties (Welte et al., 1997). Based on these properties, temperature and pressure evolution as well as generation and migration of hydrocarbons can be calculated (Welte and Yukler, 1981). The study was performed using the PetroMod TecLink v11 (SP4) software developed by the Schlumberger PetroMod Group. Complex tectonic environments like thrust belts need to be restored structurally and kinematically in order to take mass movements into account. In the present study several balanced paleo-sections were used to forward-model the temperature and maturity history of the section. With the block concept, the TecLink finite element simulator is able to handle multiple z-values on one vertical grid line. Hence each paleo-section is split into several blocks specified by its boundaries and a characteristic layer stack.

4.2.1 MODEL INPUT

The conversion of a coherent geological concept into numerical form is the precondition for basin modeling (Welte and Yalcin, 1988). To process the evolution of the basin by the si-

mulator it has to be subdivided into uninterrupted and discrete sequences, named events (Wygrala, 1988) or paleo-sections. An event is a time span during which a geological process (deposition, erosion, hiatus) occurs. The array of the software allows the discrimination of different geological processes in various parts of the basin at the same time. Physically existing sedimentary units at a certain time are called layers. Each layer is deposited during a single event and may be partly or completely eroded during a later erosional event (Wygrala, 1988). The model in this study comprises numerous original layers. Based on core analysis, facies was assigned to each layer, carrying different properties like porosity and thermal conductivity (Tab. 2). Calculations of physical properties are based on Hantschel and Kauerauf (2009). As thermal conductivity values for the rock matrix are shown in Table 2, it is important to note that porosity affects thermal conductivity to an important degree because pore fluids have lower thermal conductivities than rock matrix. A decompaction routine is integrated by default in PetroMod in order to reconstruct the initial thickness of each layer from present day data. As this function is software-related not applicable for the TecLink tool, compaction of autochthonous sediments was first computed in a preliminary model where thrusting was simulated by increasing thickness of the nappes through time (using Schlumberger PetroMod's Salt movement tool). The achieved information on compaction rates was later integrated in the thermal basin model built with the TecLink tool.

The Oligocene Schöneck, Dynow and Eggerding formations as well as the lower part of the Zupfing Formation are considered to be the source rocks (Schulz et al., 2002; Sachsenhofer et al., 2010). Because of scaling problems caused by limited thicknesses of these layers, the three formations are merged to one source rock interval in the model. The entire interval has a net thickness of approximately 70 to 100 m and is featured with an initial TOC of 2 % and a Hydrogen Index (HI) of 450 mg HC/g TOC (Schulz et al., 2002; Sachsenhofer et al., 2010). Conversion of kerogen to hydrocarbons is driven by temperature and time dependent kinetic reaction proces-

Lithostratigraphic unit	Litho mixture ratio [%]	Thermal conductivity (matrix)	
		[W/(mK)] at 20 °C	[W/(mK)] at 100 °C
Basin fill			
Innviertel Group	40 Sandst./40 Shale/20 Marl	2.48	2.07
Hall Fm.	60 Siltst./20 Sandst./20 Marl	2.37	2.03
Up. Puchkirchen Fm.	40 Siltst./40 Marl/20 Shale	1.97	1.89
Low. Puchkirchen Fm.	40 Shale/40 Marl/20 Siltst.	1.86	1.85
Source rock interval	75 Shale/25 Marl	1.91	1.86
Eocene Sandst. (reservoir rock)	80 Sandst./10 Limest./10 Marl	3.75	2.52
Mesozoic			
Cretaceous	90 Marl/10 Sandst.	2.17	1.96
Jurassic	40 Limest./40 Dolom./20 Sandst.	3.79	2.54
Thrust			
Flysch	80 Shale/10 Sandst./10 Marl	1.83	1.83
North. Calc. Alps	50 Limest./50 Dolom.	3.71	2.51

TABLE 2: Assigned thermal conductivities of rock matrix (at 20 °C and 100 °C) for various facies in the model. Calculated thermal properties are based on literature published in Hantschel and Kauerauf (2009).

ses (Tissot and Welte, 1984). Thermal history in PetroMod is calculated as a steady temperature record in a source rock through time with the purpose to assess the yield of hydrocarbons. Hydrocarbon generation reactions are described in the software by a set of activation energies and an initial potential which is described by the HI. Bulk kinetic parameters comprising activation energy distribution and single frequency factor of 5 immature lower Oligocene source rocks samples from the Molasse Basin were determined at GeoForschungsZentrum Potsdam (GeoS4 GmbH) using non-isothermal open-system pyrolysis at four different laboratory heating rates (0.7, 2.0, 5.0 and 15°C/min) and a Source Rock Analyzer®. The kinetic parameters of these samples differ only slightly (Fig. 3). An appropriate kinetic data set (named Molasse kinetic) was assigned to the source rock unit. In addition a standard kerogen Type II kinetic model was applied to test the impact of different kinetic data on the model results (Burnham, 1989).

4.2.2 BOUNDARY CONDITIONS

The sediment-water-interface (SWI) temperature represents the upper boundary condition for heat transfer in the basin. Mean surface temperature values over the time are considered in PetroMod based on paleo-temperature distribution maps after Wygrala (1989). Paleo-water depth was selected according to the general interpretation of the Molasse Basin evolution (Wagner, 1996). As hydrocarbon generation shows a strong dependence on temperature and time, the heat flow evolution is a very important constraint for modeling (Tissot and Welte, 1984). Paleo heat flow values can be assessed under consideration of tectonic processes in the past. The heat flow evolution at the base of the modeled section represents the lower thermal boundary condition.

4.2.3 CALIBRATION DATA

Different temperature-sensitive parameters, such as vitrinite

reflectance R_o (reflectance under oil), formation temperature as well as sterane (20S / (20S + 20 R)) and hopane (22S / (22S + 22R)) isomerization ratios (Mackenzie et al., 1980, 1981; Mackenzie and McKenzie, 1983) were used to calibrate the thermal evolution of the basin.

Vitrinite reflectance is measured on rocks containing remnants of landplants. Only reliable data (mainly from coals) have been used for calibration in the present study. The calculation of vitrinite reflectance is based on the kinetic EASY%Ro-algorithm (Sweeney and Burnham, 1990).

Calculations of sterane and hopane isomerization ratios are based on kinetics of Rullkötter and Marzi (1989).

The RockEval pyrolysis parameter T_{max} (Espitalié et al., 1977) was used to support the validity of the measured vitrinite reflectance data. The empirical formula

$$R_o \text{ (calculated)} = 0.0180 \times T_{max} - 7.16$$

allows to convert T_{max} to reflectance (Peters et al., 2005) and can be applied for low sulfur Type II and III kerogen.

Sterane and hopane isomerization ratios and T_{max} were taken from Schulz et al. (2002), Sachsenhofer et al. (2010) and Gratzner et al. (2011).

Two different data sets were used to calibrate the present-day heat flow distribution: (1) temperature data from borehole formation tests and (2) Horner corrected bottom-hole temperatures (BHT) ("Horner-plot"; Horner, 1951). This standard approach considers the time span since circulation of the drilling fluid stopped. Uncorrected temperature data for the Horner-calculation was taken from Kamyar (2000).

All available calibration data for wells Engenfeld1, Rohr1, Bad Hall 1, Mühlgrub 1 and Molln 1 are plotted versus depth in Figure 4 (for position of wells see Figure. 1).

4.3 MIGRATION MODELS

The 2D migration modeling package of PetroMod includes different migration modeling techniques (e.g. Darcy flow, Flow

path, Hybrid; Hantschel and Kauerauf, 2009).

Different chemical and physical parameters like critical fluid saturations or relative permeabilities which are expressed by the mobility factor (mobility factor = permeability/viscosity) are used to describe transport processes through porous media. Flow path migration is a completely buoyancy driven migration method which allows fast, high-resolution modeling. However this method requires an arbitrary definition of seal/carrier and therefore represents an incomplete physical method. Darcy flow integrates all relevant physical parameters such as pVT (pressure, volume, Temperature) and requires long computer procession times (Baur, 2010).

The Hybrid migration method was applied in the present study. It combines Darcy and flow path migration methods (Hantschel et al., 2000) and was introduced to allow proper accumulation tracking through time including timing and retention issues. This technique applies the flow path method to all lithologies which have more than 100 millidarcy permeability and a higher porosity than 30 % during the evolution of the actual layer. Beyond that it applies full Darcy calculations (i.e. hydrocarbon retention) to all layers having less permeable lithologies.

Map based migration modeling was done using PetroCharge Express (another application of PetroMod). This software tool is based on a petroleum systems approach for rapid initial assessment of petroleum charge. The software basically uses the structure of a depth map to calculate drainage areas, potential migration paths and possible locations of hydrocarbon

accumulations. The buoyancy driven approach considers features which are filled to its spill point.

5 RESULTS AND DISCUSSION

To model the petroleum system in the Sierning imbricates, a kinematic forward model was performed first, based on seismic interpretation (Fig. 1). Several wells along the profile provided data for calibration of the thermal history and the kinematic model. Obtained results are considered valid for the entire main part of the Sierning imbricates.

5.1 CROSS SECTION FORWARD MODELING

In order to model the petroleum system in the Sierning imbricates we use the results from retro-deformation (Hinsch, 2013) and further elaborate them in a regional kinematic, pseudo-dynamic forward model (Fig. 5).

10 time-deformation increments reflect the kinematic evolution of the Sierning imbricates since Middle Oligocene times (~30 Ma). Thus, the forward modeled section covers a longer time span and consequently accommodates more shortening than the balanced section of Hinsch (2013).

Total tectonic shortening in the forward modeled section is 48.5 km [L₀-L] (L= deformed length, L₀= undeformed length), corresponding to 69% of shortening (measured from the assumed hinterland end of the Penninic-Flysch and Helvetic wedge, excluding some shortening in the Northern Calcareous Alps). Note, that Figure 5 does not show the whole deformation

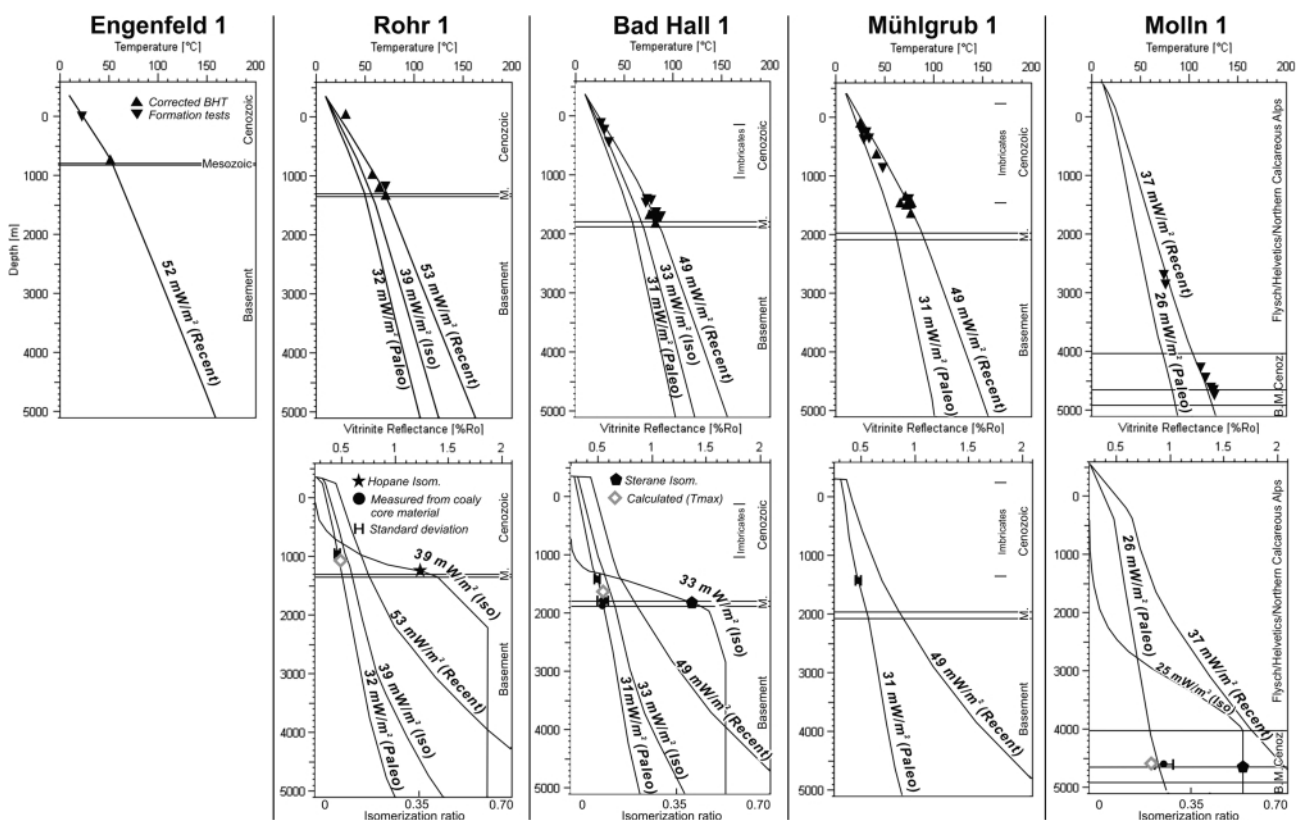


FIGURE 4: Temperature and maturity (vitrinite reflectance, steranes isomerization, hopanes isomerization) plots versus depth. En1 is the northernmost well, Mo 1 the southernmost well. Calculated trends of different heat flow scenarios are shown by different lines.

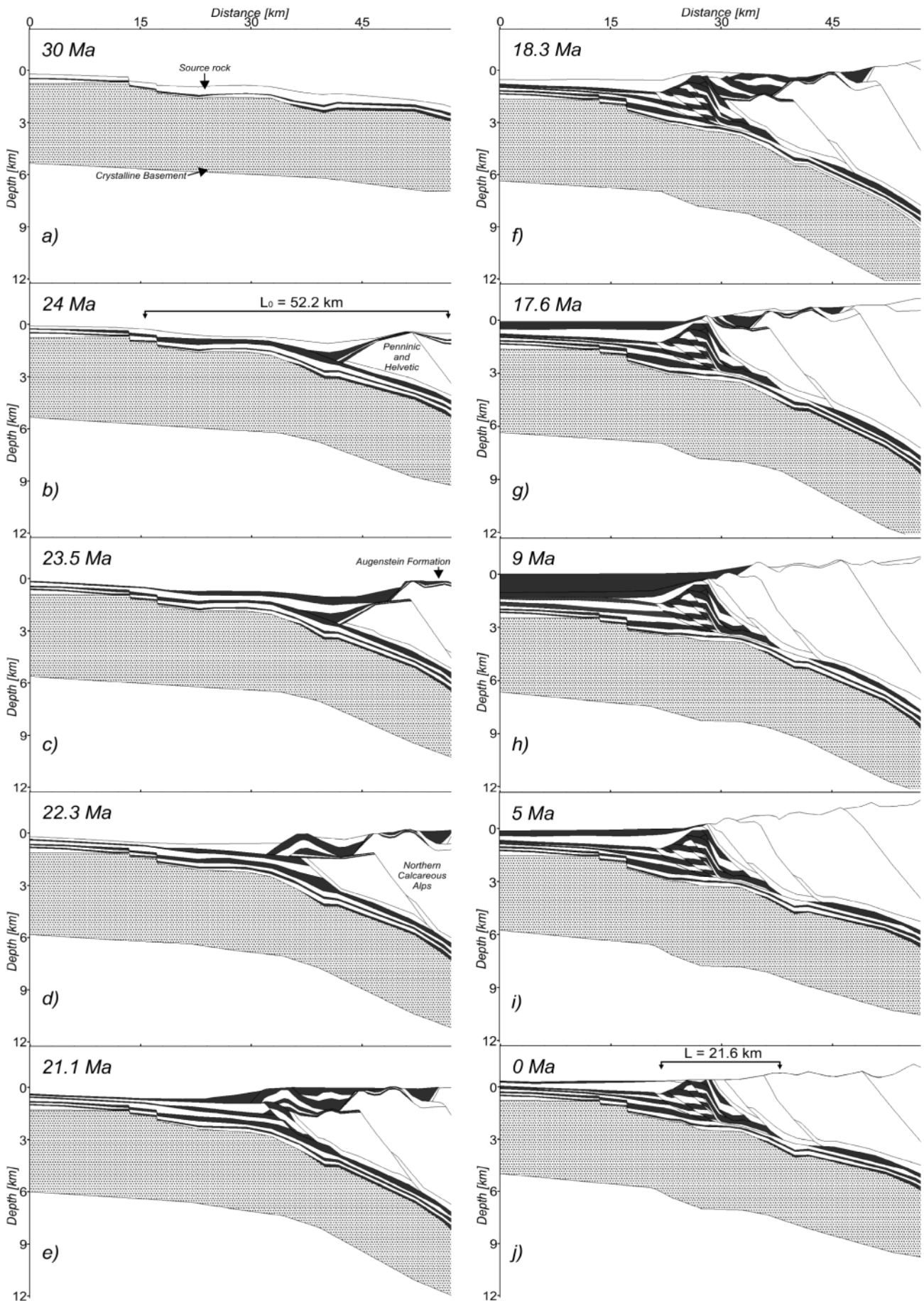


FIGURE 5: 2D basin evolution shown on a N-S section in the Sierning imbricates area (see Fig. 1). The length between reference points for calculation of tectonic shortening is displayed on Fig. 5b as well as on the present day section (Fig. 5j; black arrows).

length as it focuses on the area of interest for the subsequent basin model. It needs to be considered that this shortening value is not a minimum shortening. Lateral orogenic movements (Linzer et al., 2002) are not considered in this study.

- a) The forward model includes some overthrusting of the orogenic wedge that is not documented in preserved frontal accreted imbricates. In addition, other imbricates are eroded.
- b) In the forward model some out-of-sequence thrusting in the Penninic-Flysch and Helvetic wedge is accommodated. The timing and amount of deformation in this unit inside the considered period is relatively poorly constrained.
- c) The position of the footwall cut-off of Oligocene sediments in Fig. 5e is loosely constrained by the presence of Oligocene sediments in Well Molln 1. In the forward model the ramp was positioned approximately 20 km south of the well.

Despite these uncertainties, it is considered, that the presented forward model sufficiently reflects the evolution of the Alpine orogenic front in the study area. This is supported by the fit of the forward model with the seismic interpretation (Fig. 1) and the balanced section of Hinsch (2013). In addition, the calculated shortening velocity for the section of 4 mm/yr (48.5 km shortening in 12 m.y.) fits well to velocities calculated by balancing. The shortening velocities calculated for the balanced profile through the Sierning imbricates are 4 mm/yr and in other sections in the imbricated Molasse 4.5-8 mm/yr (Hinsch, 2013). Beidinger and Decker (submitted) assume deformation velocities of approximately 4.6-5.2 mm/yr in a comparable area for the Egerian to Karpatian period.

Thus, to conclude, the present forward model is considered to reflect the structural evolution of the frontal orogenic system in an adequate way for subsequent basin modeling.

5.2 THERMAL MODELING

5.2.1 HEAT FLOW SCENARIOS

Different heat flow scenarios were applied in the calibration process to model the thermal history along the section (Fig. 6).

In a first scenario (Fig. 6; base case 'paleo'), a time constant heat flow decreases from north to south from 32 mW/m² to 26

mW/m². This scenario results in a fit with measured vitrinite reflectance data, but underestimates present-day temperatures.

In the second scenario (base case 'recent'), heat flow decreases from north to south from 52 to 37 mW/m². This scenario results in a good fit with corrected bottom hole and formation test temperatures, but overestimates vitrinite reflectance data. Vitrinite reflectance calculated from Tmax was available for wells Rohr 1, Bad Hall 1 (middle part of the section) and Molln 1 (southernmost well) and fits to case 'paleo'. Isomerization data was available for the same wells. However, because steranes isomerization in Molln 1 reached the equilibrium value (0.50), only data from wells Rohr 1 and Bad Hall 1 in the middle part of the section can be used for heat flow calibration. The attempt to integrate these results in the actual scenarios shows that the heat flow scenario 'isomerization data fit' represents only slightly higher values than the base case 'paleo'.

Given the gap between the cases 'paleo' and 'recent', a fit for both maturity and present-day temperature data was gained by accepting the 'paleo' case heat flows until the time of maximum burial (9 million years) in order to meet the maturity data and by using the increased 'recent' heat flow for the last 4 million years.

5.2.2 SENSITIVITY ANALYSIS

Although a sub-recent increase in heat flow in the Molasse Basin has been described previously (e.g. Sachsenhofer, 2001; Gusterhuber et al., in press), it is difficult to decide whether it is a fact or artificial. Therefore, different aspects which may bias heat flow reconstructions are considered within the frame of sensitivity analysis.

5.2.2.1 CALIBRATION DATA QUALITY

Paleo-heat-flow is calibrated with measured and calculated vitrinite reflectance data applying the EASY%Ro algorithm. Recent heat flow is calibrated using measured formation temperature values. This means that apart from geological reasons, discrepancies between paleo- and present-day heat flows may occur due to biased vitrinite and temperature data or due to inaccuracies of the applied algorithm. In order to exclude the

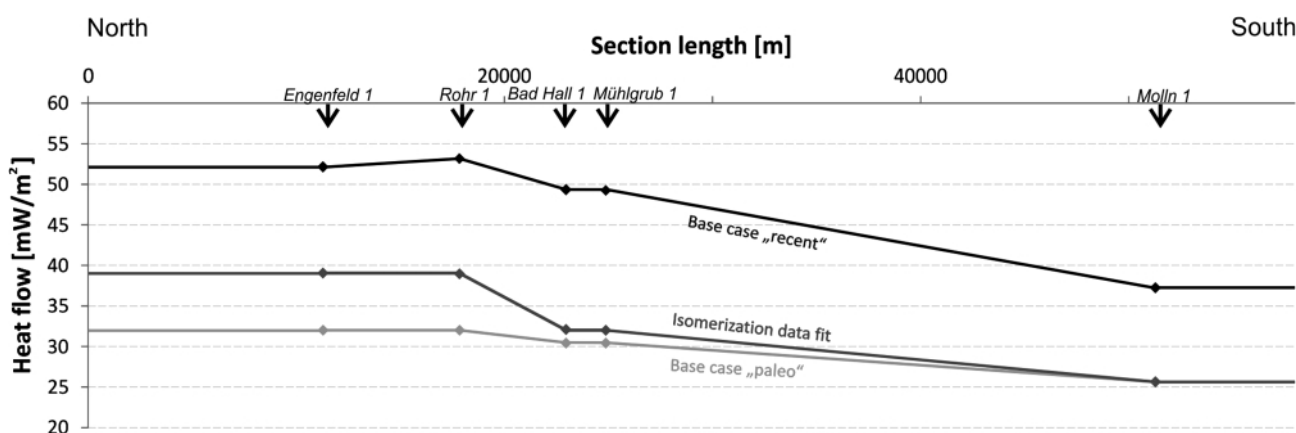


FIGURE 6: Assigned heat flow scenarios along the section. The scenario applied for petroleum systems modeling is a combination of the base cases 'paleo' and 'recent' (see text for discussion.).

probability that the low paleo-heat flow is due to biased vitrinite data (e.g. Carr, 2000), several samples were re-measured. These samples yielded identical results and did not show indications of suppression. In addition, measured vitrinite data are supported by vitrinite reflectance calculated using T_{max} values.

Temperature data derived from formation test measurements are considered highly reliable and are available from all wells. Measured bottom hole temperatures (BHT) temperatures have been corrected using the approach of Horner (1951). The corrected BHT temperatures fit reasonably well with formation test measurements, but in some cases slightly underestimate formation test temperatures. This agrees with the observation of Hermanrud et al. (1990) that the Horner plot method generally underestimates formation temperatures, if the time since circulation stopped is limited. In any case, the higher present-day heat flows are obviously not due to biased temperature data.

5.2.2.2 EFFECT OF EROSION ESTIMATES ON RE-CONSTRUCTED THERMAL HISTORIES

Significant uplift and erosion affected the Northern Calcareous Alps (Frisch et al., 2001) and the Alpine Foreland Basin during the Neogene (Gusterhuber et al., 2012). The adopted thickness of eroded rocks influences paleo-heat flow estimates and, consequently, the amount of the sub-recent heat flow increase. In order to test the possibility to eliminate the heat flow increase, absolute minimum amounts of eroded thickness have been adopted in the sensitivity analysis for wells Bad Hall 1 (located within the Molasse imbricates) and Moln 1 (located ~30 km south of the Alpine front in the Northern Calcareous Alps; see Fig. 1c for position). In case of Moln 1 also the effect of a maximum estimate was tested.

Bad Hall 1: Based on Gusterhuber et al. (2012), erosion of sediments, 1200 m thick (800 m Freshwater Molasse + 400 m Innviertel Group), has been adopted in the conceptual model (Fig. 7). Considering this assumption, a good fit with calibration data is obtained using a sub-recent heat flow increase of 18 mW/m² (Fig. 7a). In a sensitivity run, erosion was set to a minimum value of only 400 m. Even in this scenario time-constant heat flows cannot yield good fits with both, present-day temperatures and maturity. Figure 7b shows this for a time-constant heat flow of 42 mW/m², which tends to underestimate present-day temperatures, but overestimates maturity.

Moln 1: According to Frisch et al. (2001), thermochronological data suggest a maximum thickness of the Augenstein Formation in the Dachstein area (~ 50 km further west of the study area) of more than 1300 m (or even more than 2000 m). However, the thickness near the present eastern margin of the Northern Calcareous Alps was probably much lower. The current altitude in the Mo1 area is ~590 m, adjacent mountain summits reach heights between 1200 m (Reichraminger Hintergebirge) and 2200 m (Haller Mauern). Considering these facts, erosion of 2000 m (Northern Calcareous Alps + Augenstein Formation) has been adopted in the conceptual model resulting in a sub-recent heat flow increase of 11 mW/m² (Fig.

8a). Similar to Bad Hall 1, even in scenarios with a thickness of eroded rocks considered as a minimum estimate (1200 m Northern Calcareous Alps + Augenstein Formation) heat flow has to be increased by 7 mW/m² (Fig. 8b). In an additional scenario the eroded section was 2500 m thick (maximum estimate) resulting in a sub-recent heat flow increase of 14 mW/m² (Fig. 8b).

5.2.3 DISCUSSION OF HEAT FLOW HISTORY

5.2.3.1 PRESENT-DAY HEAT FLOW

According to our models, present-day heat flow varies between 37 and 52 mW/m². This range is lower than that indicated in a heat flow map of Europe (Majorowicz and Wybraniec, 2011) for the same area (50-70 mW/m²). Majorowicz and Wybraniec (2011) have shown that glaciation may have led to a substantial reduction in temperature at shallow depth (mainly <1 km) resulting in an underestimation of present-day heat flow. However, not even the southernmost (Alpine) parts of the study area were affected by Pleistocene glaciation (Van Husen, 1987). Moreover, the lowest present-day heat flows (37 mW/m²) are based on highly reliable formation test data from more than 3 km depth in the Moln 1 well. Thus, glaciation probably has no significant effect on the reconstructed present-day heat flow. Moreover, the application of paleoclimatic corrections would enlarge the difference between Neogene and present-day heat flow. In contrast, the difference between model-based present-day heat flow and the heat flow in the Majorowicz and Wybraniec (2011) map may be caused by different assessments of thermal conductivities. Predefined conductivities provided by the software have been used in this study in case of lack of measured data.

5.2.3.2 OLIGOCENE AND MIOCENE HEAT FLOW

Reconstructed Oligocene and Miocene heat flows are rather low (26-32 mW/m²) resulting in low average paleo-geothermal gradients of approximately 23 °C/km. Similar conditions have been observed in wells in the Swiss (Rybach, 1984; Schegg, 1994; Schegg and Leu, 1996; Schegg et al., 1997), German (Jacob and Kuckelkorn, 1977; Teichmüller and Teichmüller, 1986) and Austrian Molasse Basin and its fold-and-thrust belt (Sachsenhofer, 2001; Gusterhuber et al., in press).

5.2.3.3 PLIOCENE AND PLEISTOCENE INCREASE IN HEAT FLOW

Sensitivity analyses suggest that the increase in heat flow is not an artifact. However geological reasons are still poorly understood and include (see also Gusterhuber et al., in press).

- changes in hydrodynamics caused by a Pleistocene change in the stress field (Schmidt and Erdogan, 1993, 1996; Horvath and Cloetingh, 1996),
- topography-induced perturbation of the isotherms e.g. due to high exhumation rates in the Eastern Alps. However, present-day exhumation rates are clearly below values which are considered to affect the shape of isotherms (450 m/mio. year; Glotzbach et al., 2009) and

Bad Hall 1

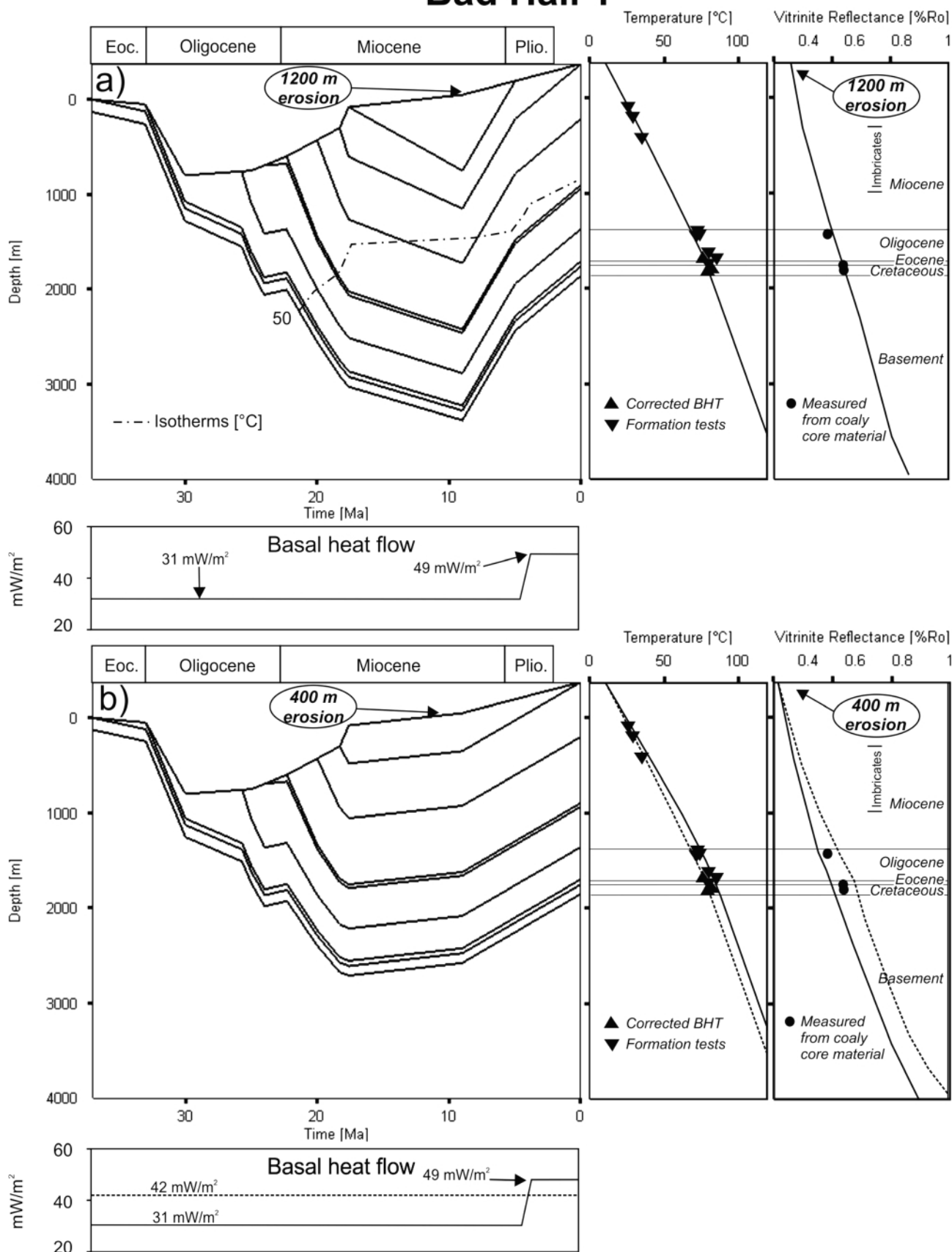


FIGURE 7: (a) Burial history of borehole Bad Hall 1 (see Fig. 1 for position) based on the input parameters from the 2D conceptual model including erosion of rocks, 1200 m thick. A combination of heat flow base cases 'paleo' and 'recent' (Fig. 6) results in a good fit between measured and calculated calibration data. (b) Burial history plot considering erosion of rocks, 400 m thick. Calibration data show that a time-constant heat flow of 42 mW/m² overestimates maturity. This result indicates that even if an unrealistic low thickness of eroded rocks is applied, a time-constant heat flow does not result in a successful fit.

Molln 1

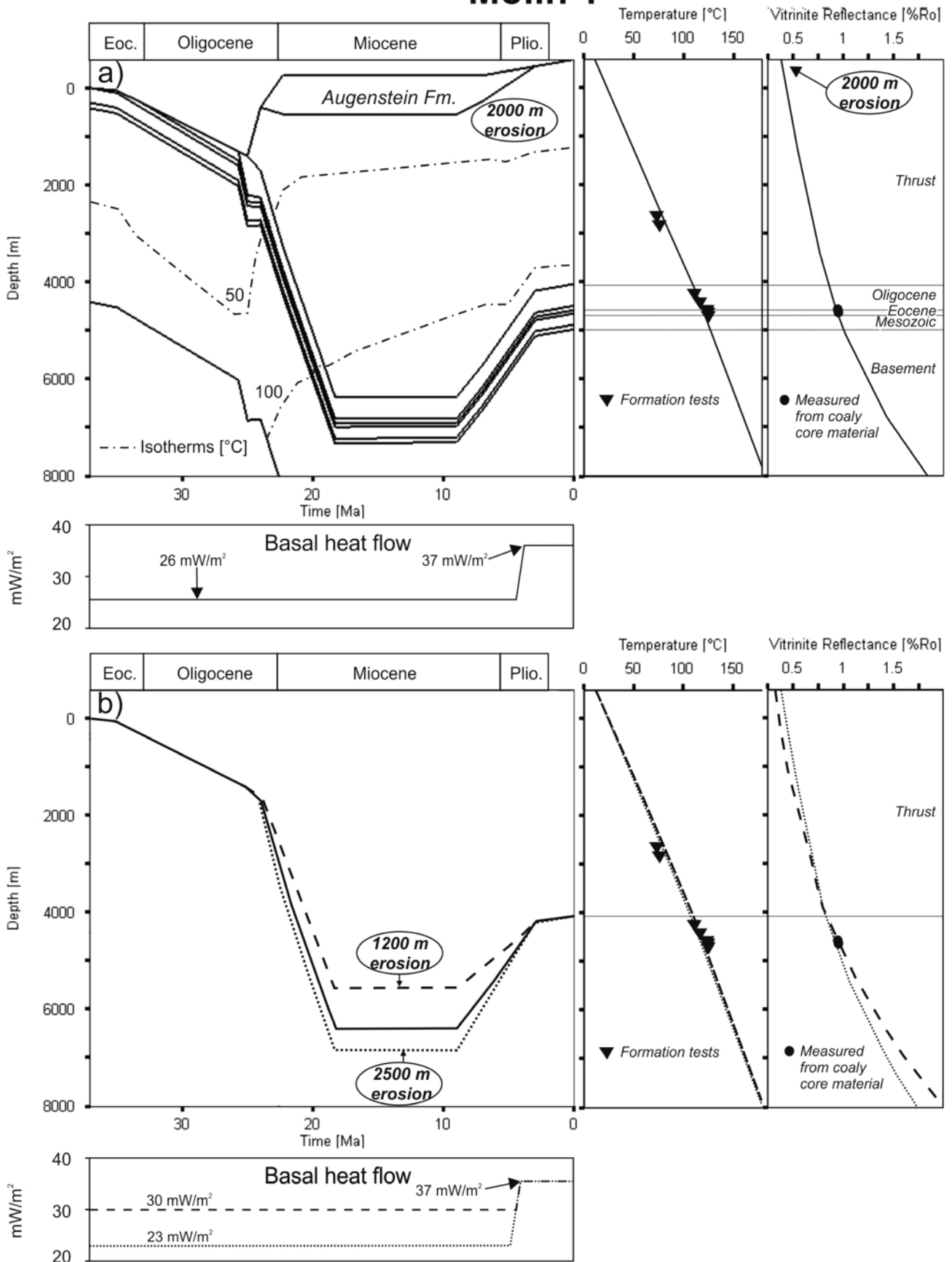


FIGURE 8: (a) Burial history of borehole Mo1 (see Fig. 1 for position) based on the input parameters from the 2D conceptual model including erosion of rocks, 2000 m thick. A combination of heat flow base cases 'paleo' and 'recent' (Fig. 6) results in a good fit between measured and calculated calibration data. (b) Burial history plots considering extremely low (1200 m) and high (2500 m) thicknesses of eroded rocks. Calibration data show that even in the scenario with minor erosion, a heat flow increase during Pliocene time has to be assumed.

- a large scale increase in mantle heat flow, which should have affected major parts of the Alps. Without more and better heat flow data from the central Eastern Alps, the latter possibility remains pure speculation.

5.2.3.4 SOUTHWARD DECREASE IN HEAT FLOW

Both, reconstructed paleo-heat flow and present-day heat flow decrease towards the south. Similar heat flow patterns have also been observed by Rybach (1984) in the Swiss, Teichmüller and Teichmüller (1986) in the Bavarian as well as Sachsenhofer (2001) and Gusterhuber et al. (in press) in the Austrian part of the Molasse Basin, respectively. The southward decrease in heat flow may have different causes: (I) thermal disequilibrium due to down-bending and thickening of the earth crust (Teichmüller and Teichmüller, 1986); (II) a thermal blanketing effect driven by the fast approach of the already compacted nappe system; (III) deep infiltration of cold surface water in the karstified rocks of the NCA (Wessely, 1983); (IV) elevated heat flows in the northern part of the Molasse Basin due to heat transfer by northward migrating fluids from beneath the Alpine nappes (Schmidt and Erdogan, 1993, 1996) which influenced the temperature field in the upper few kilometers of the crust (Rybach, 1984); (V) or any combination of the above.

5.3 PETROLEUM SYSTEMS MODELING

Bulk kinetic data determined for immature source rocks in the Austrian part of the Alpine Foreland Basin ('Molasse kinetic'; Fig. 3) and the most likely heat flow scenario (combination of heat flow base cases 'paleo' and 'recent' involving an increase in heat flow for the last 4 million years BP; Fig. 6) have been used to model hydrocarbon generation and migration.

5.3.1 HYDROCARBON GENERATION

As this study focuses on location and timing of hydrocarbon

generation, Figure 9 shows enlargements of the specific area of interest. In this figure, generation zones based on calculated vitrinite reflectance (early oil generation: 0.55-0.70 % Ro; main oil generation: 0.70-1.00 %Ro) are shown for three different time stages (22.3 Ma, 18.3 Ma, present-day). Although vitrinite reflectance isolines (red lines) cross all rock units, color codes are shown exclusively for source rock units. In addition, temperature, maturity and hydrocarbon generation histories are shown in Figure 9 for the source rock unit at three different sites: X (beneath present day imbricates); Y (beneath present day Flysch wedge), Z (present day location of Mo1).

Figure 9 shows that at 22.3 Ma the studied section was still immature. Between 22.3 and 18.3 Ma deep burial due to (on-going) overthrusting resulted in a strong increase in temperature at all studied sites (X: 95°C; Y: 115°C; Z: 135°C). Consequently the early and main oil windows are reached at sites Y and Z, respectively. Nevertheless, the calculated transformation ratio suggests that minor hydrocarbons (<20 % of the total potential) have been generated at site Z. Till 7 million years BP site Y reached the main oil window and additional hydrocarbons have been generated at sites Y and Z. Later uplift and erosion resulted in cooling and terminated hydrocarbon generation.

The calculated transformation ratio at site Z is 38 %. This value fits well with the observed average HI of the source rock unit in well Moln 1, which is about 285 mgHC/gTOC (Gratzer et al., 2011) and thus 30 to 52 % lower than that of immature equivalents (400-600 mgHC/gTOC; Table 1).

5.3.2 SENSITIVITY ANALYSIS

Correlations of geophysical well logs suggest that in the area east of the Lindach Fault the source rock facies north of the Alpine nappes and in the sub-thrust subthrust is identical (Sachsenhofer and Schulz, 2006). Thus it is useful to apply

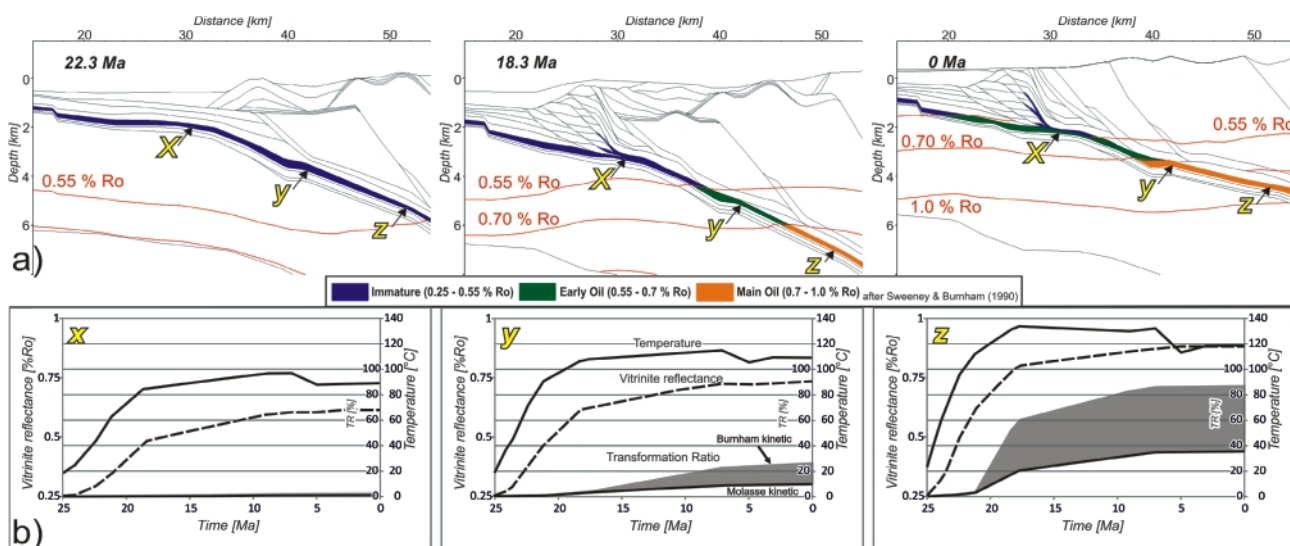


FIGURE 9: Petroleum generation beneath the Alpine nappes. (a) Generation zones at different time-slices. Red lines indicate the boundaries between different maturity stages. (b) Time plots showing the evolution of temperature, vitrinite reflectance and the transformation ratio (TR) over time for three different sites (X, Y, Z) under the thrust belt. Grey shaded areas mark the difference in TR between the 'Molasse kinetic' and the kinetic data set for Type II kerogen of Burnham (1989).

the 'Molasse kinetic' data set. However, to study the sensitivity of the study results to different kinetic data sets, an alternative kinetic data set (Type II kerogen of Burnham, 1989; Fig. 3) was considered for sensitivity analysis. The comparison between the calculated transformation ratios shows that the timing of hydrocarbon generation is similar. However, more generated hydrocarbons (higher transformations ratios) are predicted using the Burnham (1989) kinetics (e.g. 82 vs. 32 % for site Z).

5.3.3 HYDROCARBON CHARGE

5.3.3.1 2D MIGRATION MODEL

In Figure 10, four representative time steps (18.3, 9.0, 5.0 Ma and present day) of the modeled 2D section were chosen to illustrate hydrocarbon migration from the oil kitchen below the Alpine nappes towards the foreland.

The time step of 18.3 Ma (Fig. 10) was selected because it represents a time of major hydrocarbon generation beneath the Alpine wedge (see site X in Fig. 9). At 18.3 Ma years, the migrating liquid hydrocarbons (green arrows) reached a position between Ro1 and En1. The model shows that oil migrated along the source rock interval until it reached a fault juxtaposing the Lower Oligocene source rock interval against Cenomanian and Eocene reservoir units (see also migration models in Malzer et al., 1993). The presence of oil fields proves that relevant faults have acted as migration pathways at least at certain times. Since exact times are unknown, an intermediate time-constant shale gouge ratio of 50 % was set for the faults in the model to allow at least part-time migration. This fault type is expressed by a shale ratio with regard to the offset lithologies. Typical values are 35 % (low shale content) for relatively permeable faults or 70 % (high shale content) for relatively impermeable faults. Typical early stage liquid hydrocarbon accumulations apparently occurred at this time in the fault bounded block between Bad Hall 1 and Mühlgrub 1. Minor gas was generated at 18.3 Ma. According to the model, gas migrated at a relatively higher stratigraphic position and partly diffuses into overlying low-permeability layers (Zupfing Formation; red arrows).

The time step of 9 Ma is close to the supposed time of maximum burial and shortly before the termination of hydrocarbon generation (Fig. 9). Liquid and gaseous hydrocarbons continued to migrate northward. A small oil accumulation is predicted near the northern well Wels Ost 1.

Because of considerable uplift between 9 Ma and present day (Gusterhuber et al., 2012), almost no hydrocarbons were generated during the late stage evolution of the sub-thrust (Fig. 9). However, significant re-migration occurred along the section. Important model results include:

- 1) Long-distance northward migration of liquid hydrocarbons.
Long-distance migration is also supported by oil seeps near the northern basin margin west of Linz (Gratzer et al., 2012) proving tens of kilometers of lateral migration.
- 2) Migration of (thermogenic) gas along fault zones into Molasse imbricates. This may be a consequence of uplift and

erosion causing a significant pressure drop in the subsurface. Actually minor thermogenic gas has been found in biogenic gas accumulations in the Sierning imbricates (Pytlak, pers. comm., 2013).

- 3) Apparent vertical migration indicated by saturations of thermogenic gas into the Puchkirchen and Hall formations. Vertical diffusive migration of thermogenic gas (and condensate) and mixing with biogenic gas accumulations in the Puchkirchen and Hall formations have been described by Reischenbacher and Sachsenhofer (2011).

5.3.3.2 'PSEUDO 3D' MIGRATION MODEL

Fig. 11 shows structure maps of the main reservoir horizons: Cenomanian and Eocene (base Oligocene in areas where Eocene sediments are missing). The maps were compiled using the 3D seismic volume (see outline in Fig. 1) and were extended to the south and north considering 2D seismic and well data in order to include the oil kitchen and hydrocarbon accumulations located north of the 3D seismic volume. The northern boundary of the oil kitchen is defined by the 0.6 % Ro reflectivity isoline (Linzer and Sachsenhofer, 2010).

A very rough estimate of the total hydrocarbon volume migrating from the sub-thrust area to the foreland can be derived from the source potential index (SPI) of the Lower Oligocene succession (~1 ton hydrocarbon/m² surface; Sachsenhofer et al., 2010), the kitchen area (~100 x 20 km), the average density of Molasse oil (850 kg/m³ corresponding to an API grade of 35; Gratzer et al., 2011) and losses during primary migration in the order of 25 %. This assessment gives a volume in the order of 11 billion barrels of oil (BBO).

To be conservative, a total volume of 7 BBO was injected close to the northern boundary of the oil kitchen (0.6 % Ro) into Cenomanian (3.5 BBO) and Eocene horizons (3.5 BBO) in order to visualize migration pathways in the foreland (Fig. 11).

As expected, modeled migration pathways are northward trending (Fig. 11). Some oil migrates across the northern model border and may cause oil seeps detected at the basin margin (Gratzer et al., 2012). Several hydrocarbon fields with Cenomanian and/or Eocene reservoir units are predicted by the model. These include the large Voitsdorf field and a number of smaller fields (e.g. Redltal, Hiersdorf, Kemating; Fig. 11). Other major fields with Cenomanian (e.g. Trattnach) and Eocene reservoirs (e.g. Sattledt, Ried) are not clearly predicted by the models. In contrast a number of fields are predicted in the western part of the study areas, where no commercial oil has been found yet.

Models are useful, both if they make a fit or a misfit with observations. In this case, it is obvious that part of the mismatch is related to low model resolution outside of the 3D cube and the fact that present-day structure maps instead of paleo-structures maps (e.g. 9 Ma, time of main migration pulse; see Fig. 9) have been used. Moreover, facies changes and pressure regimes are not considered in the simple flow path approach. Apart from that, we see two main reasons for the mismatch, which are discussed below:

1) Sachsenhofer and Schulz (2006) and Gusterhuber et al. (in press) emphasized that source rocks in the western part of the study area have been removed by tectonic erosion and

are now found in the Molasse imbricates. This suggests, together with the model results that the absence of petroleum fields in the western sector of the basin is a consequence

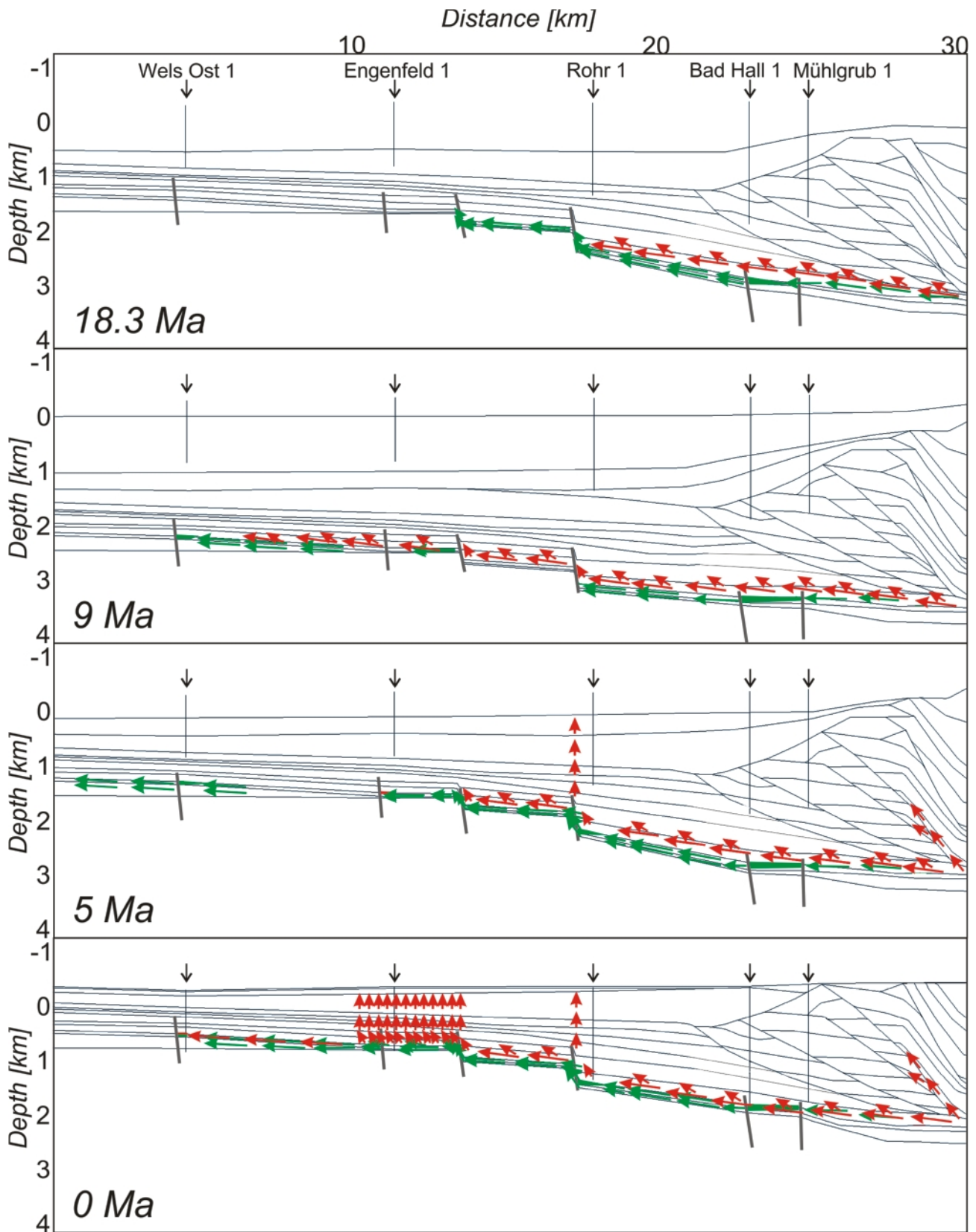


FIGURE 10: 2D migration model (see Fig. 1 for location). Green (for liquids) and red (for gas) arrows indicate migration pathways based on calculated hydrocarbon saturations at certain time steps. Little patches having the same color coding indicate possible petroleum accumulations.

are now found in the Molasse imbricates. This suggests, together with the model results that the absence of petroleum fields in the western sector of the basin is a consequence of missing charge rather than of missing structures.

- 2) Migration probably did not only occur within the major carrier beds, but seemingly also along major fault systems

These results look plausible but however some uncertainties have to be considered. Although the best resolution available from the 3D seismic volume was used, parts off the 3D coverage were interpolated and may be too smooth to chase the exact location of reservoirs. Another uncertainty may be caused by the fact that present day but not paleo maps were used.

Present day maps are only able to show the actual migration, not migration at the time of initiation. In addition, important factors like facies behaviors and pressure regimes are not considered in these migration models. Unfortunately, existing data of the area which includes the oil kitchen is very sparse. 3D seismic data is limited to the foreland and there are only a few wells drilled in this part. However, this preliminary work provides a proper basement for further studies.

5.3.4 BIODEGRADATION RISK

Fig. 12a shows a plot of API gravity of Molasse oils versus depth. The plot indicates that biodegraded oils, characterized

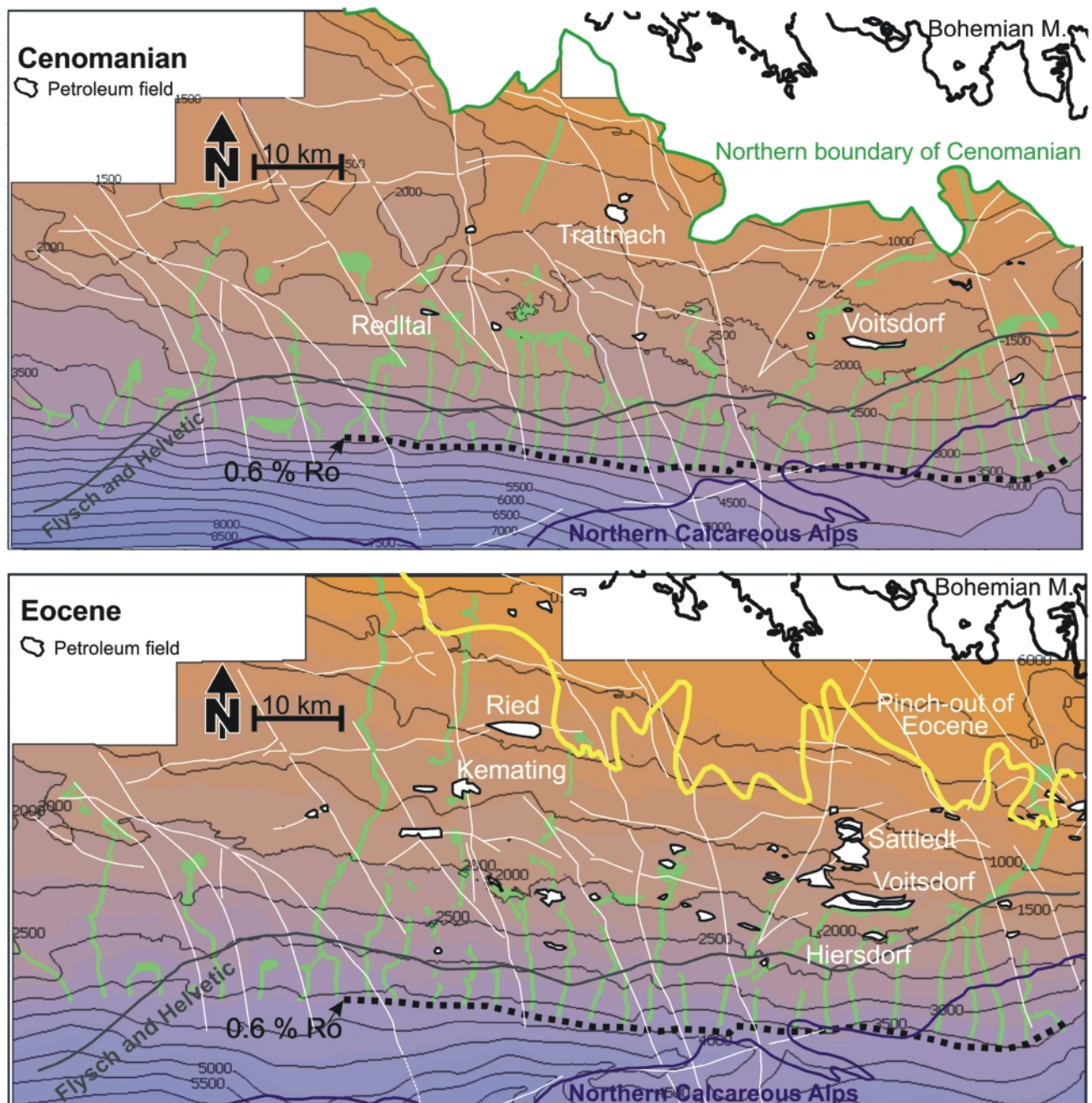


FIGURE 11: Depth structure maps representing Upper Cretaceous and Eocene carrier/reservoir horizons. The dotted 0.6 % Ro iso-reflectivity represents a rough assessment of the oil kitchen boundary. Bright green traces and batches show possible simulated oil migration pathways and accumulations, respectively. Petroleum fields and fault patterns (white lines) are shown in each horizon.

by API grades <30, are restricted to shallow levels (<800 m sub-sea) with present-day temperatures $\leq 50^\circ$ (see also Gratzner et al., 2011). At first sight the shallow threshold depth for biodegradation in the study area is astonishing, because bacteria responsible for biodegradation are known to occur up to 80°C (e.g. Head et al., 2003).

The lack of biodegraded oil at greater depth may be explained by the 'palaeopasteurization' model (Wilhelms et al., 2000), postulating that petroleum reservoirs were pasteurized at $80\text{--}90^\circ\text{C}$, inactivating any hydrocarbon-degrading microorganisms present, during deep burial before the main oil charge and subsequent uplift of the reservoir to cooler conditions.

The 2D model is used to test the applicability of the 'palaeopasteurization' model in the Alpine Foreland Basin. In Fig. 12b the position of the 80°C isotherm along the northern sector of the modeled cross-section is shown for the time of maximum burial (9 Ma). Different grey shadings indicate the upward increasing risk for biodegradation. In Fig. 12c the present day situation is shown together with the paleo- 80°C isotherm. The depth interval between the paleo- and the present-day 80°C isotherm has been affected by 'palaeopasteurization'. The present-day position of the paleo- 80°C isotherm is at about 1 km below sea level fitting reasonable well with the observed depth of biodegradation. Thus 'palaeopasteurization' may have a positive effect on the preservation of hydrocarbons in the Alpine Foreland Basin.

Important to note, that the 'palaeopasteurization' model is only applicable if most hydrocarbons migrated into shallow reservoirs after maximum burial. Although some oil reached petroleum traps in the northern part of the cross-section (e.g. Wels Ost 1) already during maximum burial (9 Ma), Figure 10 shows that additional oil accumulated during (5 Ma) and after uplift (present-day).

6 CONCLUSIONS

- The presented structural model is a kinematic model with geodynamic background and provides an appropriate input for the petroleum systems model. It supposes that total tectonic shortening in the modeled section is at least 48.5 km which corresponds to 69 % of shortening (mainly in the Molasse sediments, including some limited shortening in the Penninic-Flysch and Helvetic wedge but excluding shortening of the Northern Calcareous Alps).
- Maturity data indicate rather low paleo-heat flows along the modeled section decreasing from north to south from 32 to 26 mW/m^2 (base case 'paleo'). Formation temperatures indicate present-day basal heat flows decreasing in the same direction from 52 to 37 mW/m^2 (case 'recent'). Consequently, a heat flow scenario which involves a sub-recent (~ 4 Ma BP) increase in heat flow from base case 'paleo' to base case 'recent' is accepted as most likely. This heat flow history is similar to that reconstructed for a

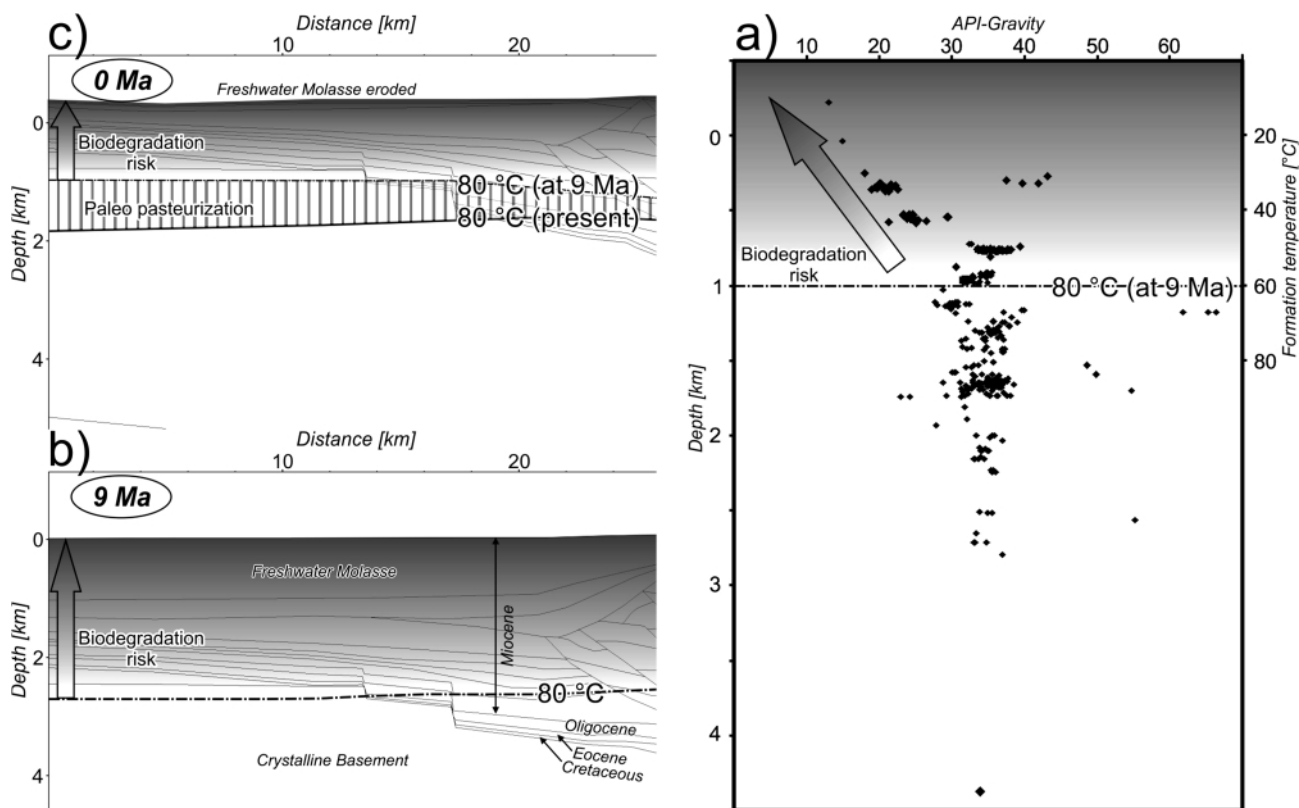


FIGURE 12: (a) Plot of API gravity of Molasse oils versus depth. Biodegraded oils with low API grades occur at shallow depth (above 800 m sub-sea) corresponding to present formation temperatures of about 50°C . (b) Modeled 80°C isotherms in the northern part of the 2D section for the time of maximum burial (9 Ma). Grey shading indicates the upward increasing biodegradation risk. (c) Modeled 80°C isotherms in the northern part of the 2D section for present-day (0 Ma). The position of the paleo- 80°C isotherm is also shown.

parallel cross-section through the Perwang imbricates (~90 km west of the present cross-section) by Gusterhuber et al. (in press).

- The above heat flow history and bulk kinetic data from Oligocene source rocks have been used for petroleum systems modeling. According to these models, hydrocarbon generation commenced at about 18 Ma (Early Miocene) due to deep burial beneath Alpine nappes and was terminated about 8 Ma (Late Miocene) due to cooling caused by uplift and erosion. Whereas the sub-thrust area beneath the Flysch wedge remained immature, about 40 % of the total source potential was realized beneath the Northern Calcareous Alps in the MolIn 1 area.
- Hydrocarbon migration commenced contemporaneously with hydrocarbon generation, but continued until present day. Main model results include: (1) Oil migrated along the source rock interval till it reached faults with sufficient vertical throw to allow hydrocarbon migration into stratigraphically deeper reservoir units; (2) Long-distance (>50 km), lateral, northward migration of oil (and gas); (3) Migration of gas along fault zones into the Sierning imbricates; (4) Apparent vertical diffusive migration of gas into the Oligo-/Miocene Puchkirchen and Hall formations. Detected and producing hydrocarbon deposits in Cenomanian and Eocene horizons (e.g. Malzer et al., 1993), oil seeps along the northern basin margin (Gratzer et al., 2012), mixtures of biogenic and thermogenic gas in the Sierning imbricates and the Puchkirchen and Hall formations (Reischenbacher and Sachsenhofer, 2011) show that the model results fit well with observations.
- A flow path approach for modeling migration pathways in the main carrier/reservoir units ('Pseudo 3D Model') produces ambiguous results. Whereas some major petroleum fields are successfully predicted, others are not. Moreover, accumulations are predicted in areas, where no hydrocarbons have been detected yet. Apart from model simplifications, the mismatch reflects the absence of source rocks in the western part of the study area (e.g. Sachsenhofer and Schulz, 2006) as well as the important role of fault zones for hydrocarbon migration.
- The applied 2D model suggests that deep burial (9 Ma) and subsequent uplift to cooler conditions (Gusterhuber et al., 2012) resulted in 'palaeopasteurization' of reservoirs near the northern basin margin. This model may explain that biodegradation in the Austrian part of the Alpine Foreland Basin is limited to the depth interval down to 800-1000 m sub-sea.

ACKNOWLEDGEMENTS

The authors thank RAG AG for their kind permission to publish the data. The used software PetroMod was generously granted as academic license by the Schlumberger Technology Center, Aachen, Germany. We would also like to thank Doris Gross, Reinhard Gratzer and Achim Bechtel (Montanuniversität Leoben) for providing a wealth of appropriate geochemical data.

REFERENCES

- Baur, F., 2010. Quantification of heat and fluid flow through time by 3D modeling: an example from the Jeanne d'Arc basin, offshore eastern Canada. PhD thesis, RWTH Aachen, 170 p.
- Beidinger, A. and Decker, K., submitted. Quantifying Early Miocene in-sequence and out-sequence thrusting at the Alpine-Carpathian junction. *Tectonics*.
- Bernhardt, A., Stright, L. and Lowe, D.R., 2012. Channellized debris-flow deposits and their impact on turbidity currents: the Puchkirchen axial channel belt in the Austrian Molasse Basin. *Sedimentology*, 59, 7, 2042-2070.
- Burnham, A.K., 1989. A simple kinetic model of petroleum formation and cracking. Lawrence Livermore National Laboratory Report, UCID-21665, 11 p.
- Carr, A.D., 2000. Suppression and retardation of vitrinite reflectance, part 1. Formation and significance for hydrocarbon generation. *Journal of Petroleum Geology*, 23, 313-343.
- Covault, J.A., Hubbard, S.M., Graham, S.A., Hirsch, R. and Linzer, H.-G., 2009. Turbidite-reservoir architecture in complex foredeep-margin and wedge-top depocenters, Tertiary Molasse foreland basin system, Austria. *Marine and Petroleum Geology*, 26, 379-396.
- De Ruig, M.J. and Hubbard, S.M., 2006. Seismic facies and reservoir characteristics of a deep marine channel belt in the Molasse foreland basin. *AAPG Bulletin*, 90, 735-752.
- Dohmann, L., 1991. Die unteroligozänen Fischeschiefer im Molassebecken. Ph.D. thesis, Ludwig Maximilian Universität, München, 365 pp.
- Espitalié, J., LaPorte, J.L., Madec, M., Marquis, F., Leplat, P., Poulet, J. and Boutefeu, A., 1977. Méthode rapide de caractérisation des roches mères de leur potentiel pétrolier et de leur degré d'évolution. *Revue de l'Institut Français du Pétrole*, 32, 23-42.
- Frisch, W., Kuhlemann, J. and Dunkl, I., 2001. The Dachstein paleosurface and the Augenstein Formation in the Northern Calcareous Alps – a mosaic stone in the geomorphological evolution of the Eastern Alps. *International Journal of Earth Sciences*, 90, 500-518.
- Genser, J., Cloetingh, S.A.P.L., Neubauer, F., 2007. Late orogenic rebound and oblique Alpine convergence: New constraints from subsidence analysis of the Austrian Molasse basin. *Global and Planetary Change*, 58, 1-4, 214-223.
- Glotzbach, C., Spiegel, C., Reinecker, J., Rahn, M. and Frisch, W., 2009. What perturbs isotherms? An assessment using fission-track thermochronology and thermal modelling along the Gotthard transect, Central Alps. *Geological Society of London, Special Publications*, 324, 111-124.

- Gratzer, R., Bechtel, A., Sachsenhofer, R.F., Linzer, H.-G., Reischenbacher, D. and Schulz, H.-M., 2011. Oil-oil and oil-source rock correlations in the Alpine Foreland Basin of Austria: Insights from biomarker and stable carbon isotope studies. *Marine and Petroleum Geology*, 28, 1171-1186.
- Gratzer, R., Schmid, C. and Stanzel, A.I., 2012. Bewertung und Abgrenzung eines natürlichen Ölaustrittes im Eferdinger Becken. *Beiträge zur Hydrogeologie*, 59, 203-217.
- Grunert, P., Soliman, Coric A., S. Rötzel, R. Harzhauser, M. and Piller, W.E., 2012. Facies development along the tide-influenced shelf of the Burdigalian Seaway: An example from the Ottnangian stratotype (Early Miocene, middle Burdigalian). *Marine Micropaleontology*, 84-85, 14-36.
- Grunert, P., Hinsch, R., Sachsenhofer, R.F., Bechtel, A., Coric, S., Harzhauser, M., Piller, W.E. and Sperl, H., 2013. Early Burdigalian infill of the Puchkirchen Trough (North Alpine Foreland Basin, Central Paratethys): facies development and sequence stratigraphy. *Marine and Petroleum Geology*, doi:http://dx.doi.org/10.1016/j.marpetgeo.2012.08.009.
- Gusterhuber, J., Dunkl, I., Hinsch, R. Linzer, H.-G. and Sachsenhofer, R.F., 2012. Neogene uplift and erosion in the Alpine Foreland basin (Upper Austria and Salzburg). *Geologica Carpathica*, 63, 295-305.
- Gusterhuber, J., Hinsch, R. and Sachsenhofer, R.F., in press. Evaluation of hydrocarbon generation and migration in the Molasse fold and thrust belt (Central Eastern Alps, Austria) using structural and thermal basin models. *AAPG Bulletin*.
- Hantschel, T., Kauerauf, A., Wygrala, B., 2000. Finite element analysis and ray tracing modeling of petroleum migration. *Marine and Petroleum Geology*, 17, 7, 815-820.
- Hantschel, T. and Kauerauf, A., 2009. *Fundamentals of Basin Modeling*. Springer Verlag, 425 p.
- Head, I.M., Jones, D.M. and Larter, S.R., 2003. Biological activity in the deep subsurface and the origin of heavy oil. *Nature*, 426, 344-352.
- Hermanrud, C., Cao, S. and Lerche, I., 1990. Estimates of virgin rock temperature derived from BHT measurement: Bias and errors. *Geophysics*, 55 (7), 924-931.
- Hinsch, R., 2008. New Insights into the Oligocene to Miocene Geological Evolution of the Molasse Basin of Austria. *Oil & Gas European Magazine*, 34 (3), 138-143.
- Hinsch, R. and Linzer, H.-G., 2010. Along-strike variations of structural styles in the Imbricated Molasse of Salzburg and Upper Austria: A 3D seismic perspective. *European Geosciences Union General Assembly, Geophysical Research Abstracts*, 12, EGU2010-4966-3.
- Hinsch, R., 2013. Laterally varying structure and kinematics of the Molasse fold and thrust belt of the Central Eastern Alps: implications for exploration. *AAPG Bulletin*, 97, 10, 1805-1831.
- Horner, D.R., 1951. Pressure buildup in wells, in: Brill, E.J. (Ed.), *Proceedings of the Third World Petroleum Congress. The Hague Section II, Cologne*, 503-521.
- Horvath, F. and Cloetingh, S., 1996. Stress-induced late-stage subsidence anomalies in the Pannonian basin. *Tectonophysics*, 266, 287-300.
- Hubbard, S.M., De Ruig, M.J. and Graham, S.A., 2005. Utilizing outcrop analogs to improve subsurface mapping of natural gas-bearing strata in the Puchkirchen Formation, Molasse Basin, Upper Austria. *Austrian Journal of Earth Sciences*, 98, 52-66.
- Hubbard, S.M., De Ruig, M.J. and Graham, S.A., 2009. Confined channel-levee complex development in an elongate depositor: Deep-water Tertiary strata of the Austrian Molasse basin. *Marine and Petroleum Geology*, 26, 85-112.
- Jacob, H. and Kuckelkorn, K., 1977. The carbonization profile of the Miesbach 1 well and its oil geological interpretation. *Erdöl-Erdgas-Zeitschrift*, 93, 115-124.
- Kamyar, H. R., 2000. Verteilung der Untergrundtemperaturen an den Beispielen der Bohrlochtemperatur (BHT) – Messungen in den RAG – Konzessionen Oberösterreichs und Salzburgs, (Molasse- und Flyschzone). PhD-thesis, University of Vienna, Austria, 145 pp.
- Krenmayr, H. G., 1999. The Austrian sector of the North Alpine Molasse: A classic foreland basin. *FOREGS (Forum of European Geological Surveys) Dachstein-Hallstatt-Salzkammergut Region, Vienna*, 22-26.
- Kuhlemann, J. and Kempf, O., 2002. Post-Eocene evolution of the North Alpine Foreland Basin and its response to Alpine tectonics. *Sedimentary Geology*, 152, 45-78.
- Linzer, H.-G., 2001. Cyclic channel systems in the Molasse foreland basin of the Eastern Alps - the effects of Late Oligocene foreland thrusting and Early Miocene lateral escape. *AAPG Bulletin*, 85, 118 (abstract).
- Linzer, H.-G., 2002. Structural and stratigraphic traps in channel systems and intraslope basins of the deep-water molasse foreland basin of the Alps. *AAPG 2002 Annual Convention & Exhibition, Houston, Texas*.
- Linzer, H.-G., Decker, K., Peresson, H., Dell'Mour, R. and Frisch, W., 2002b. Balancing lateral orogenic float of the Eastern Alps. *Tectonophysics*, 354, 211 –237.
- Linzer, H.-G., 2009. Gas in Imbricated Channel Systems of the Foreland Basin of the Eastern Alps (Austria). *AAPG 2008 Annual Convention & Exhibition San Antonio, Texas*.

- Linzer, H.-G. and Sachsenhofer, R.F., 2010. Submarine Large Scale Mass Movements in the Deepwater Foreland Basin of the Alps - Implications to Hydrocarbon Generation and Distribution of Source and Reservoir Rocks. AAPG 2010 Annual Convention & Exhibition New Orleans.
- Mackenzie, A.S., Patience, R.L., Maxwell, J.R., Vandenbroucke, M. and Durand, B., 1980. Molecular parameters of maturation in the Toarcian shales, Paris basin, France - I: changes in the configurations of acyclic isoprenoid alkanes, steranes and triterpanes. *Geochimica et Cosmochimica Acta*, 44, 1709-1721.
- Mackenzie, A.S., Hoffman, C.F. and Maxwell, J.R., 1981. Molecular parameters of maturation in the Toarcian shales, Paris basin, France - III: changes in aromatic steroid hydrocarbons. *Geochimica et Cosmochimica Acta*, 45, 1345-1355.
- Mackenzie, A.S. and McKenzie, D., 1983. Isomerization and aromatization of hydrocarbons in sedimentary basins formed by extension. *Geology Magazine*, 120, 417-470.
- Majorowicz, J. and Wybraniec, S., 2011. New terrestrial heat flow map of Europe after regional paleoclimatic correction application. *International Journal of Earth Sciences*, 100, 881-887.
- Malzer, O., Rögl, F., Seifert, P., Wagner, L., Wessely, G. and Brix, F., 1993. Die Molassezone und deren Untergrund. In: F. Brix and O. Schultz (eds.), *Erdöl und Erdgas in Österreich*. Naturhistorisches Museum Wien und F. Berger, 281-358.
- Nachtmann, W., 1995. Fault-bounded structures as hydrocarbon traps in the upper Austrian Molasse Basin. *Geologisch Paläontologische Mitteilungen Innsbruck*, 20, 221-230.
- Peters, K.E., Walters, C.C. and Moldowan, J.M., 2005. The biomarker guide, 2nd ed. Cambridge University Press, 1155 pp.
- Reischenbacher, D. and Sachsenhofer, R., 2011. Entstehung von Erdgas in der oberösterreichischen Molassezone: Daten und offene Fragen. *BHM*, 156 (11), 463-468.
- Röder, D. and Bachmann, G., 1996. Evolution, structure and petroleum geology of the German Molasse Basin, In: P. Ziegler and F. Horvath, (eds.), *Peri-Tethys Memoir 2, Structure and Prospects of Alpine Basins and Forelands*. *Mémoire du Muséum National d'Histoire naturelle*, 170, 263-284.
- Rögl, F., 1998. Paläogeographic Considerations for Mediterranean and Paratethys Seaways (Oligocene to Miocene). *Annales des Naturhistorischen Museums in Wien*, 99A, 279-310.
- Rullkötter, J. and Marzi, R., 1989. New aspects of the application of sterane isomerization and steroid aromatization to petroleum exploration and the reconstruction of geothermal histories of sedimentary basins. Reprint Division of Petroleum Geochemistry, American Chemical Society, 34, 126-131.
- Rybach, L., 1984. The paleogeothermal conditions of the Swiss Molasse Basin: Implications for hydrocarbon potential. *Rev. Institut Français Du Pétrole*, 39, 143-146.
- Sachsenhofer, R. F., 2001. Syn- and post-collisional heat flow in the Cenozoic Eastern Alps: *International Journal of Earth Sciences*, 90, 579-592.
- Sachsenhofer, R.F. and Schulz, H.-M., 2006. Architecture of Lower Oligocene source rocks in the Alpine Foreland Basin: a model for syn- and post-depositional source - rock features in the Paratethyan realm. *Petroleum Geoscience*, 12, 363-377.
- Sachsenhofer, R.F., Leitner, B., Linzer, H.-G., Bechtel, A., Coric, S., Gratzner, R. Reischenbacher, D. and Soliman, A., 2010. Deposition, Erosion and Hydrocarbon Source Potential of the Oligocene Eggerding Formation (Molasse Basin, Austria). *Austrian Journal of Earth Sciences*, 103, 76-99.
- Sachsenhofer, R.F., Linzer, H.-G., Bechtel, A., Dunkl, I., Gratzner, R., Gusterhuber, J., Hinsch, R. and Sperl, H., 2011. Influence of Alpine Tectonics on Source Rock Distribution, Hydrocarbon Generation and Migration in the Austrian Part of the Molasse Basin. AAPG 2011 International Conference and Exhibition, Milan, Italy.
- Schegg, R., 1994. The coalification profile of the well Weggis (Sub-alpine Molasse, Central Switzerland): Implications for erosion estimates and the paleogeothermal regime in the external part of the Alps. *Bulletin Swiss Association of Petroleum Geol. and Engineers*, 61, 57-67.
- Schegg, R. and Leu, W., 1996. Clay mineral diagenesis and thermal history of the Thonex well, western Swiss Molasse Basin. *Clays and Clay Minerals*, 44 (5), 693-705.
- Schegg, R., Leu, W., Cornford, C. and Allen, P. A., 1997. New coalification profiles in the Molasse Basin of Western Switzerland: Implications for the thermal and geodynamic evolution of the Alpine Foreland. *Eclogae Geologicae Helvetiae*, 90, 79-96.
- Schmidt, F. and Erdogan, L. T., 1993. Basin modelling in an overthrust area of Austria. In: A.G. Doré, E. Holter, J.H. Augustson, W. Fjeldskaar, S. Hanslien, Ch. Hermanrud, B. Nyland, D. J. Stewart and O. Sylta, (eds.), *Basin Modelling: Advances and Applications*. NPF Special Publications, 3, 573-581.
- Schmidt, F. and Erdogan, L. T., 1996. Paleohydrodynamics in exploration. In: W. Liebl and G. Wessely, (eds.), *Petroleum exploration and production in thrust belts, foreland basins and orogenic basins*. European Association of Petroleum Geologists Special Publications, 5, 255-265.
- Schulz, H.-M., Sachsenhofer, R.F., Bechtel, A., Polesny, H. and Wagner L., 2002. Origin of hydrocarbon source rocks in the Austrian Molasse Basin (Eocene-Oligocene transition). *Marine and Petroleum Geology*, 19, 683-709.
- Schulz, H.-M., Bechtel, A., Rainer, T., Sachsenhofer R.F. and Struck, U., 2004. Paleoceanography of the western central paratethys during nannoplankton zone NP 23. The Dynow Marlstone in the Austrian Molasse Basin. *Geologica Carpathica*, 55, 311-323.

- Schulz, H.-M. and van Berk, W., 2009. Bacterial methane in the Atzbach-Schwanenstadt gas field (Upper Austrian Molasse Basin), Part II: Retracing gas generation and filling history by mass balancing of organic carbon conversion applying hydrogeochemical modelling. *Marine and Petroleum Geology*, 26, 1180-1189.
- Schulz, H.-M., van Berk, W., Bechtel, A., Struck, U. and Faber, E., 2009. Bacterial methane in the Atzbach-Schwanenstadt gas field (Upper Austrian Molasse Basin), Part I: Geology: *Marine and Petroleum Geology*, 26, 1163-1179.
- Sissingh, W., 1997. Tectonostratigraphy of the North Alpine Foreland Basin: Correlation of Tertiary depositional cycles and orogenic phases. *Tectonophysics*, 282, 223-256.
- Steininger, F.F., Wessely, G., Rögl, F. and Wagner, L., 1986. Tertiary sedimentary history and tectonic evolution of the Eastern Alpine foredeep. *Giornale di Geologia Bologna*, 48 (3), 285-297.
- Sweeney, J.J. and Burnham, A.K., 1990. Evaluation of a simple model of vitrinite reflectance based on chemical kinetics. *AAPG Bulletin*, 74, 1559-1570.
- Teichmüller, R. and Teichmüller, M., 1986. Relations between coalification and paleogeothermics in variscan and alpidic foredeeps of western Europe. *Lecture Notes in Earth Sciences*, 5, 53-80.
- Tissot, B.P. and Welte, D.H., 1984. *Petroleum Formation and Occurrence*. 2nd ed., Springer-Verlag, Berlin, 699 pp.
- van Husen, D., 1987. Die Ostalpen in den Eiszeiten. Populärwissenschaftliche Veröffentlichungen der Geologischen Bundesanstalt, Vienna, Map, scale 1:500,000.
- Veron, J., 2005. The Alpine Molasse Basin – Review of petroleum geology and remaining potential. *Bulletin für Angewandte Geologie*, 10, 75-86.
- Wagner, L.R., 1996. Stratigraphy and hydrocarbons in the Upper Austrian Molasse Foredeep (active margin). In: G. Wessely and W. Liebl (eds.), *Oil and Gas in Alpidic Thrustbelts and Basins of Central and Eastern Europe*. EAGE Special Publications, 5, 217-235.
- Wagner, L.R., 1998. Tectono-stratigraphy and hydrocarbons in the Molasse foredeep of Salzburg, Upper and Lower Austria. In: A. Mascle, C.Puigdefàbregas, H.P.Luterbacher and M.Fernandez (eds.), *Cenozoic Foreland Basins of Western Europe*. Geological Society, Special Publications, 134, 339-369.
- Welte, D. H. and Yukler, M. A., 1981. Petroleum origin and accumulation in basin evolution - A quantitative model. *AAPG Bulletin*, 65, 1387-1396.
- Welte, D. H. and Yalcin, M.N., 1988. Basin modelling - A new comprehensive method in petroleum geology. *Organic Geochemistry*, 13, 141-151.
- Welte, D. H., Horsfield, B. and Baker, D.R., 1997. *Petroleum and Basin Evolution*. Springer Verlag, 535 p.
- Wessely, G., 1983. Zur Geologie und Hydrodynamik im südlichen Wiener Becken und seiner Randzone. *Mitteilungen der österreichischen Geologischen Gesellschaft*, 76, 27-68.
- Wilhelms, A., Larter, S.R., Head, I., Farrimond, P., di-Primio, R. and Zwach, C., 2000. Biodegradation of oil in uplifted basins prevented by deep-burial sterilisation. *Nature*, 411, 1034-1037.
- Wygrala, B., 1988. Integrated computer-aided basin modeling applied to analysis of hydrocarbon generation history in a Northern Italian oil field. *Organic Geochemistry*, 13, 187-197.
- Wygrala, B., 1989. Integrated study of an oil field in the southern Po Basin, northern Italy. PhD thesis, University of Cologne, 226pp.

Received: 16 October 2013

Accepted: 12 December 2013

Jürgen GUSTERHUBER¹⁾²⁾, Ralph HINSCH³⁾⁴⁾, Hans-Gert LINZER³⁾ & Reinhard F. SACHSENHOFER¹⁾

¹⁾ Montanuniversität Leoben, Department Applied Geosciences and Geophysics, Chair of Petroleum Geology, Peter-Tunner-Straße 5, A-8700 Leoben, Austria;

²⁾ Present address: SANTOS Ltd., 60 Flinders Street, Adelaide SA 5000, Australia;

³⁾ RAG Rohöl-Aufsuchungs Aktiengesellschaft, Schwarzenbergplatz 16, A-1015 Vienna, Austria;

⁴⁾ Present address: OMV Exploration & Production GmbH, Trabrennstraße 6-8, 1020 Vienna;

^{*)} Corresponding author, juergen.gusterhuber@santos.com